RADIATION LEVELS IN BUILDING MATERIALS ALONG KANGUNDO ROAD, NAIROBI CITY COUNTY, KENYA

AMOSI NYONGESA CHILAI, (BED (SC))

I56/CE/15643/2005

A Thesis Submitted in Partial Fulfillment of the Requirements for the Award of the Degree of Master of Science (Physics) in the School of Pure and Applied Sciences of Kenyatta University

April, 2025

DECLARATION

This thesis is my original work and has never been presented for the award of a degree or any other award in any institution of higher learning.

Amosi Nyongesa Chilai Signature:  Date 23/04/2025

156/CE/15643/2005

Department of Physics

Kenyatta University

SUPERVISORS:

This thesis was submitted with our approval as University Supervisors.

Dr. Nadir O. Hashim Signature:  Date 23/04/2025

Department of Physics

Kenyatta University

Dr. Felix Wanjala Omonya Signature  Date 23/04/2025

International Atomic Energy Agency (IAEA)

Vienna, Austria

DEDICATION

I dedicate the Thesis to my father; Festo Chilai Mmbaka, my wife Esther Ondego, and my children.

ACKNOWLEDGEMENTS

I would like to thank Drs. Felix Wanjala Omonya and Nadir Hashim, my two supervisors, for their constant moral and academic help. I am appreciative of Kenyatta University's Physics Department for helping to make this research successful by providing laboratory space, ICT services for accessing scientific journals, and knowledgeable technical staff. Special thanks to Mr. Wataka for his assistance in the laboratory. Thank you to the technician for supplying informative reading materials. I express gratitude to my fellow Kenyatta University students, especially Kenneth Amukah and Veronica, for their moral and academic assistance. Appropriately, I also express my gratitude to the Research Assistants who worked diligently to help us achieve reproducible results, and also acknowledge the support of all my family and friends from the start to the end of this research work. Most importantly, I am grateful to God for giving me good health, energy and determination that has made it possible for me to complete my research work.

TABLE OF CONTENTS

LIST OF TABLES

LIST OF FIGURES

ABBREVIATIONS AND ACRONYMS

I_S	Intensity of the Sample
H_{ex}	External Hazard Index
D	Absorbed dose in air
As	Specific activity of the sample
AEDR	Annual Effective Dose Rate
ADC	Analogue to Digital Converter
UV	Ultraviolet
UNSCEAR	United Nations Scientific Committee on Effects of Atomic Radiations
TENORM	Technological Enhanced Natural Occurring Radionuclide
RPB	Radiation Protection Board
Ra_{eq}	Radium equivalent activity
PMT	Photomultiplier tube
OECD	Organization for Economic Cooperation and Development
NRS	Natural Radiation Sources
NaI (T1)	Thallium activated sodium iodide
M_S	Mass of the Sample
MCB	Multichannel Buffer
MCA	Multichannel Analyzer
IAEA	International Atomic Energy Agency
E_y	Photon Energy
Z	Number of Electron
ROI	Region of Interest
FWHM	Full Width Half Maximum
KNRA	Kenya Nuclear Regulatory Authority
NORM	Naturally Occurring Radioactive Material

ADRA	Absorbed dose rates in air
WHO	World Health Organization
ICRP	International Commission on Radiological Protection
HPGE	High Purity Germanium
MeV	Mega Electron Volt
GPS	Global Positioning System

ABSTRACT

The primary contributor to human exposure to ionizing radiation is from Natural Radiation Sources (NRS). This type of radiation comes mainly from terrestrial sources and accounts for a significant portion of the radiation humans receive on a daily basis. Terrestrial radiation is emitted from naturally occurring radioactive materials in the Earth's crust, such as radon gas, uranium, thorium, and potassium. To date, there has been no investigation into the concentration of radioactivity in construction materials found along Kangundo Road in Nairobi City County. This research aimed at assessing the environmental impact and human exposure to ionizing radiation from building materials found along Kangundo road in Nairobi. A purposive random sampling method was deployed in this work to collect samples of building materials for analysis. The radioactivity concentration levels in the sampled building materials were determined using a NaI(TI) spectrometer at Kenyatta University laboratory. The activity concentrations measured for ^{40}K ranged from 151 ± 8 to 2392 ± 120 Bq/kg, while ^{238}U exhibited values between 27 ± 2 and 412 ± 21 Bq/kg, and ^{232}Th showed a range from 54 ± 3 to 612 ± 31 Bq/kg. The radioactivity levels for most of the radionuclides exceeded the global average values of 420 Bq/Kg, 33 Bq/kg, and 45 Bq/Kg for ^{40}K, ^{238}U, and ^{232}Th respectively. The absorbed dose rate was found to vary from 65 ± 3 to 616 ± 31 $nGyh^{-1}$, which remains below the international safety threshold of 1500 $nGyh^{-1}$. The Radium Equivalent values were recorded between 138.18 ± 7 Bq/Kg and 1344 ± 67 Bq/Kg, with sample K3 presenting the highest Radium Equivalent value, surpassing the global safety limit of 370 Bq/Kg. The annual effective dose rate exhibited a range from 0.16 ± 0.01 $mSvy^{-1}$ to 1.51 ± 0.02 $mSvy^{-1}$, with the highest measurement recorded in sample K3, surpassing the globally accepted maximum dose limit of 1 $mSvy^{-1}$. This elevated annual effective dose rate may be attributed to the samples being sourced from regions characterized by a significant presence of igneous rocks. The computed Gamma index (Hazard Index) values for the samples varied, with a minimum of 0.31 ± 0.02 $mSvy^{-1}$ and a maximum of 3.63 ± 0.14 $mSvy^{-1}$, where six samples exceeded the permissible safety threshold of 1 $mSvy^{-1}$. The average Hazard Index determined in this study was calculated to be 1.01 ± 0.08 $mSvy^{-1}$ which is within the range of world permissible limit of 1 $mSvy^{-1}$. This study adds to our understanding of radiation exposure levels and the related health hazards for construction workers, residents, and occupants of buildings made from materials with high radiation levels.

CHAPTER ONE

INTRODUCTION

1.1 Background to the Study

Humans have always been exposed to natural radiation from the Earth throughout their lives (Mohan and Chopra, 2022). Radioactive elements with long half-lives in the Earth's lithosphere have been causing natural radioactivity since the universe was formed. These radioactive materials, especially ^{238}U, ^{232}Th, and ^{40}K, are commonly present in a wide range of geological materials such as gravels, granites, sand, and gypsum, all of which are frequently utilized in construction projects (Mohan and Chopra, 2022).

When assessing the effects of building materials on the environment and human health, radiation measurement is essential, especially when considering radioactive building materials. Knowing the dangers of using these materials and how they can harm the environment and people's health is important for building in a way that is good for the planet and our well-being. The potential health hazards linked to elevated radiation levels in building materials raise concerns, particularly in instances of high radiation and limited information on activity concentration levels in such materials. This knowledge gap highlights the necessity for conducting research on building materials utilized in Kenya, specifically in locations such as Kangundo Road, where elevated activity concentration levels are suspected due to Natural Radiation Sources (NRS). This study was prompted by Oborah's (2022) research.

His study discovered increased radiation levels in construction materials in Babadogo Nairobi County. The study aimed to find out the radiation exposure levels from building materials along Kangundo Road in Nairobi City County. The study's main goal was to assess and calculate the true risks that Kangundo Road residents would face from using construction materials with elevated radiation levels. In this study, a variety of construction materials, including sand, bricks, and concrete blocks, were selected for radioactivity assessment. To evaluate radiological risks and their effects on human health, it was essential to understand the naturally occurring radioactivity levels in these construction materials. This study will assist the Kenya Nuclear Regulatory Commission (KNRA) to come up with rules, guidelines and recommendations for safely using and managing construction materials to prevent harmful radiation exposure to people and the environment.

1.2 Statement of the Research Problem

The swift urbanization and building boom along Kangundo Road, Nairobi County, Kenya, have sparked apprehensions regarding the possible utilization of construction materials with elevated radiation levels. Although construction plays a crucial role in urban advancement, the uncontrolled utilization of such materials may result in considerable environmental and health hazards. The utilization of construction materials with heightened radiation levels could potentially contribute to environmental deterioration, encompassing soil and water pollution as a result of increased ionizing radiation exposure. This contamination possesses the potential to yield enduring repercussions on the local ecosystem.

The hazards linked to the elevated exposure to ionizing radiation encompass an increased likelihood of cancer, genetic alterations, and radiation-induced ailments (Amutallah *et al*., 2023). Despite the potential threats linked to radioactive construction materials, there exists a scarcity of local data and investigations on the prevalence, categories, and radiation levels in these materials employed in construction along Kangundo Road. This knowledge gaps impedes well-informed decision-making and the establishment of suitable regulations and guidelines to safeguard individuals and the environment against exposure to the ionizing radiation.

1.3 Hypothesis

The assumption of this research is that the levels of radioactivity stemming from the Natural Radiation Sources (NRS) and the effective gamma radiation exceed permissible thresholds in the construction materials utilized along the Kangundo road. This occurrence is linked to getting construction materials from certain areas characterized by geological formations rich in granite and sand sourced from nearby riverbeds in the surrounding districts, which are in close proximity to areas with elevated background radiation. Over time, farmers in these regions have introduced technologically enhanced naturally occurring radionuclides (TENORM), potentially resulting in radiation levels surpassing those recommended by the International Commission on Radiological Protection (ICRP, 2000).

1.4 Objectives of the Study

1.4.1 General Objective

The general objective of this study was to assess the human exposure and environmental impact of ionizing radiation from naturally occurring radionuclides found in building materials collected along the Kangundo road in Nairobi County, Kenya.

1.4.2 Specific Objectives

i. To calculate the concentration of Natural Radiation Sources (NRS), of ^{238}U, ^{232}Th, and ^{40}K, in building materials (sand, clay bricks, and concrete blocks) used along the Kangundo Road.

ii. To determine the environmental impact of radioactive building materials by examining their potential for soil and water contamination in the Kangundo Road area.

iii. To determine the radiation exposure levels for construction workers, residents, and occupants of buildings constructed with these materials, and assess the associated health risks.

1.5 Justification of Study

Notwithstanding the sharp rise in building activity in Kenya, there hasn't been much in-depth investigation into the existence and effects of ionizing radiation exposure in building materials.

The insufficient number of studies in this area emphasizes the necessity to investigate the potential dangers linked to the utilization of these materials containing heightened levels of

radiation. When construction materials have high levels of natural radioactive substances like uranium, thorium and radon gas, they can be harmful to human health. For instance, the inhalation or ingestion of radon gas is widely recognized as a primary cause of lung cancer. It is imperative to comprehend the occurrence of radioactive materials in construction activities along Kangundo Road to pinpoint possible health risks for both the local community and construction laborers. Additionally, the incorporation of building materials containing escalated radiation levels in construction endeavors can lead to adverse repercussions on the environment and human health. These materials might also discharge radioactive components into the ground and underground water reservoirs, thereby impacting the ecosystem and water purity. This research coupled with its findings can provide tools for cleaner energy, healthcare, environmental monitoring, and even improved resource management, all of which align with the broader goals of creating a more sustainable, equitable, and safe world.

CHAPTER TWO

LITERATURE REVIEW

2.1 Radiation Measurement

International Atomic Energy Agency (1987) found that the main sources of radiation in the environment come from nature, which account for 82% of the total, man-made sources, which account for 18%, and other sources, which contribute less than 1%. The soil, water, and air all naturally release these radionuclides. The impact of gamma radiation exposure on people is being noticed especially in homes workplaces and schools in Kenya (Mustapha, 1999). Owing to inadequate knowledge regarding the concentrations and risks associated with gamma rays, a significant number of individuals continue to reside in buildings unaware of the potential hazards posed by such radiation (Stojanovska *et al*., 2010).

Moreover, the human body assimilates these radionuclides on a daily basis through water and food in the form of chemicals. Along Kangundo Road, numerous human endeavors are ongoing, which may intensify Naturally Occurring Radioactive Materials (NORM) and lead to elevated concentrations of NORM in the area around us (Faheem *et al*., 2008).

2.2 Similar Studies on Assessment of Activity Levels as well as Gamma Index

Studies have been conducted on natural radioactivity, but there is limited research on construction materials in along Kangundo Road.

In a recent study by Oborah (2022) it was found that building materials used in Babadogo Estate in Nairobi City County Kenya have safe levels of radioactivity and radiation hazards. Hashim (2000) analyzed soil samples collected in Mombasa Kenya in 2000 to find out how much radionuclides were present ^{40}K, ^{232}Th, and ^{238}U. According to the results, the radionuclide levels were within permissible bounds.

Felix O. Wanjala (2019) discovered that the amount of radiation in the soil in Ortum Kenya was higher than the average worldwide levels. This could potentially increase the amount of radiation people are exposed to in that area. It was found that the mean ADRA at one meter above the ground was 112 ± 30 $nGyh^{-1}$. Because Ortum's soil and rocks have a terrestrial radionuclide activity concentration that is below the globally advised threshold values, it was suggested that they be used. According to a study by Osoro (2007), radioactivity was detected in the surface soil of the planned titanium mines in Kenya, showing low levels of natural radionuclide present. In Kakamega County, Kenya, in a different research study, Songa (2021) used murram as building materials and measured the levels of activity i.e., ^{226}Ra, ^{232}Th, and ^{40}K using gamma spectroscopy. The results showed the activity levels within the world acceptable safety levels. Osoro (2007) found that the amount of radiation absorbed from soil samples in Mrima Hills Kenya was about seven times higher than the safe limit set globally. In the Kyerwa District of Tanzania, research carried out at the Tin mines showed ^{226}Ra concentrations of activity were elevated in waste rock (Gurisha *et al.*, 2020).

Global research on the inherent radioactivity of Indian building materials and their by-products conducted by Viresh *et al*. (1999) demonstrated that the activity was lower than world acceptable safety limit. Different research in Turkey utilized gamma ray spectroscopy to analyze the levels of concentration ^{238}U, ^{232}Th and ^{40}K for a variety of building materials. The activity level ranged between 3.5 $Bqkg^{-1}$ and 114.1 $Bqkg^{-1}$, 1.6 $Bqkg^{-1}$ and 20.7 $Bqkg^{-1}$ then 201.4 $Bqkg^{-1}$ and 4928.8 $Bqkg^{-1}$ respectively (Mavi and Akurt, *2010)*.

In Cyprus, after applying the WHO (2012) dose criteria to superficial materials, it was found that 25 samples adhered to the 0.3mSv/y exception limit, with only one surpassing it. Stoulos *et al*. (2003) examined gamma ray radiation from commonly used natural tiling rocks at the same dose rate. The outcome revealed the level of activity of ^{232}Th ranging from 1 - 906 Bq/kg, ^{238}U from 1 - 588 Bq/kg and ^{40}K from 50 - 1606 Bq/kg. Flores *et al*. (2005) evaluated the concentration of activity in 40 samples of materials extensively used for construction in Cuba province using Gamma ray spectrometry. The results showed that the average concentration values fell within the expected range 9 Bq/kg to 857 Bq/kg^{-} in ^{40}K, 6 Bq/kg to 57 Bq/kg in ^{226}Ra and 1.2 Bq/kg to 22 Bq/kg in ^{232}Th. Using gamma ray spectroscopy, Simin *et al*., (2011) from Iran examined the natural radioactivity found in construction materials. The study's findings showed that gypsum had the lowest ^{232}Th concentration, at 2.2 Bq/kg, and cement had the highest, at 28.9 Bq/kg.

The research indicated that cement samples exhibited maximum concentrations of ^{226}Ra at 39.6 Bq/kg and ^{232}Th at 28.9 Bq/kg. Conversely, the gypsum samples recorded their lowest concentrations at 2.2 Bq/kg for ^{232}Th and 8.1 Bq/kg for ^{226}Ra. The hazard index derived from this study remained below the suggested thresholds, with a dose rate measured at 53.7 nGy/y.

2.3 Human Health and Radiation

There have been two sources of background radiation since the formation of the earth: radiation from the earth and cosmic rays from space. According to Melission (1966), naturally occurring radioactive forms of potassium, uranium, and thorium as well as terrestrial radiations are generated on Earth. Building materials with radioactive elements like uranium, thorium, and potassium have been utilized in construction for many years and can be harmful to health when exposure is at high levels. These materials have the potential to release high levels of radiation, which could have a negative impact on human health if they are used in construction (Abdullahi *et al*., 2022). Commonly used radioactive building materials such as granite and natural stones have varying levels of radioactive isotopes, mainly uranium and thorium.

Other forms of radioactive construction materials, such as bricks and concrete, have increased amounts of Natural Radiation Sources (NRS), while certain ceramic tiles may also have traces of radioactive elements. Ionizing radiation is released by these materials, primarily in the form of gamma rays.

Continued contact with these materials containing high levels of radiation may result in higher radiation doses for individuals, which could increase the likelihood of radiation-related health problems. Moreover, radon gas, a radioactive gas that is odourless and colourless, is produced by uranium and thorium and can build up inside buildings. Extended exposure to high radon levels is an established factor that raises the possibility of lung cancer (Degu Belete and Alemu Anteneh, 2021). Genetic impact is another potential health consequence from prolonged exposure to radioactive construction materials. Excessive radiation exposure can result in genetic mutations, which may then cause hereditary illnesses.

Since there is always radiation present in nature, we need to think about how it affects people's health. On average most of the radiation exposure people get comes from sources on land according to UNSCEAR's 2000 report. The average yearly dose of radiation from external sources around the world is set by the International Commission on Radiological Protection (ICRP) to protect people from harmful ionizing radiation. The Commission anticipates that the general exposure to population should not surpass an annual exposure of 1 mSv, while occupational exposure should not go beyond 20 mSv annually, excluding radiation exposure from medical and background sources (UNSCEAR, 2000).

Radiation has two types of effects: somatic and genetic. When there is a somatic effect, the person who was exposed to radiation suffers damage, while genetic effect manifests in their descendants (Dunalp, 1988). Damage from radiation is transmitted to future generations through the reproductive cells in the reproductive organs.

Long-term radiation exposure can cause health problems like cancer and leukemia, according to Baykara *et al.* (2000). Additionally, there are two categories for radiation effects: immediate and long-term. According to the International Digital Organization for Science Information (2012), immediate effects include burns and radiation sickness, which happen when high radiation doses are administered quickly. Issues such as cataract development and cancer development are examples of delayed consequences symptoms that can show up months or years after being exposed to radiation.

CHAPTER THREE

THEORETICAL BACKGROUND OF GAMMA-RAY SPECTROSCOPY

3.1 Introduction

The chapter will discuss different concepts such as gamma ray spectroscopy and the production of the gamma rays. Secular equilibrium and the way gamma rays interact with matter will also be discussed. Furthermore, there will be documentation of radiation exposure and its impact on the environment, as well as its effects on human health.

3.2 Gamma-Ray Spectroscopy

Gamma-ray spectrometry is used for qualitative and quantitative determination of radionuclides that emit gamma radiation. It includes the accurate assessment and scrutiny of gamma rays, which are high-energy photons released during nuclear transitions. The spectroscopic technique enables the detection of precise radionuclides, along with their energy levels and decay characteristics (Xu *et al*., 2020). Through the use of detectors like high-purity Germanium (HPGe) detectors, Scintillation detectors, or NaI(Tl) detectors, gamma-ray spectroscopy allows scientists to acquire energy spectra, which show distinctive peaks linked to specific gamma-ray energies. A key instrument in nuclear physics is gamma-ray spectroscopy, environmental monitoring, and radiation protection as it offers valuable information about nuclear material composition, radioactive decay nature, and radiation source quantification.

3.3 Production of Gamma Rays

One kind of high-energy electromagnetic radiation is gamma rays that is generated by different nuclear processes like nuclear decay, particle interactions, and nuclear reactions. The de-excitation of excited atomic nuclei is a key method for producing gamma rays. When a nucleus is in a higher energy state, usually due to absorbing energy or previous nuclear reactions, it can release the extra energy by giving off gamma rays. This type of gamma rays is known for having very high frequencies and energies, usually falling within the MeV range.

3.4 Secular Equilibrium

Secular equilibrium is an important aspect in nuclear physics, especially for understanding radioactive decay and the stability of radionuclides. This phenomenon happens when the daughter radionuclide is produced at the same rate it decays through the decay of its parent radionuclide. Put simply, in a secular equilibrium, the levels of parent and daughter nuclides remain steady throughout time. Due to the parent radionuclide's substantially shorter half-life than that of the daughter radionuclide, this balance is achieved.

The Bateman equation (3.1), a key equation in nuclear decay physics, is used to describe secular equilibrium.

$$N_{d(t)} = \lambda_p N_p \left(1 - e^{\frac{-\lambda_d \times t}{\lambda_d - \lambda_p}}\right), \quad (3.1)$$

where $N_{d(t)}$ indicates the quantity of daughter nuclei present at the particular moment 't.', N_p represents the original quantity of parent nuclei, λ_d is the rate at which the daughter radionuclide undergoes decay, λ_p is the decay constant for the parent radionuclide and 't' represents time.

In secular equilibrium, the daughter radionuclide's decay rate is controlled only by the parent radionuclide's activity because the daughter's creation rate matches its decay rate. As previously stated, secular equilibrium includes the activity of both the parent radionuclide and the daughter radionuclide. These two can be stated in the following manner.

3.5 Activity of the Parent Radionuclide (A_p):

The rate at which the parent radionuclide decays, known as its activity, can be determined through the equation (3.2),

$$A_p = \lambda_p \times N_p \quad (3.2)$$

where A_p refers to the parent radionuclide's activity, λ_p is the rate of decay for the parent radionuclide, N_p is the quantity of maternal nuclei.

3.6 Activity of the Daughter Radionuclide (A_d):

The daughter radionuclide's activity can be determined using the same equation (3.3):

$$A_d = \lambda_d \times N_d \quad (3.3)$$

Where A_d is the activity of the daughter radionuclide, λ_d is the rate at which the daughter radionuclide decays and N_d is the quantity of daughter nuclei.

In secular equilibrium, it is crucial for the parent and daughter radionuclides to maintain a consistent activity level throughout time. One way to represent this is by using equation (3.4),

$$A_p = A_d \tag{3.4}$$

In this balance, daughter nuclei decay at the same rate that they are formed during the decay of parent nuclei. The exponential decay law, which is described in Equation 3.5, governs the diminishing of radioactive substances as time progresses.

$$N_{(t)} = N_0 \times e^{-\lambda t} \tag{3.5}$$

Where $N_{(t)}$ is the quantity of nuclei at time 't.', N_0 is the first set of nuclei sometimes called the beginning number, λ represents the constant rate of decay and 't' symbolizes time.

These equations are crucial for comprehending and measuring the behavior of radioactive substances in construction materials, especially when studying parent-daughter radionuclide pairs and evaluating radiation levels in building materials as time passes.

3.7 Gamma Rays Interaction with Matter

Gamma rays which are high-energy photons interact with different substances in different ways each having its own special traits.

Three primary mechanisms i.e. the photoelectric effect, the Compton effect, and pair production are used by gamma rays to interact with matter. These techniques for interacting with matter and radiation are essential for measuring and detecting radiation. The energy (*hv*) of the gamma-ray and the atomic number of the materials determines the probability that any of the three processes will occur. The three mechanisms' differing dominance in relation to water interaction is shown in Figure 1.

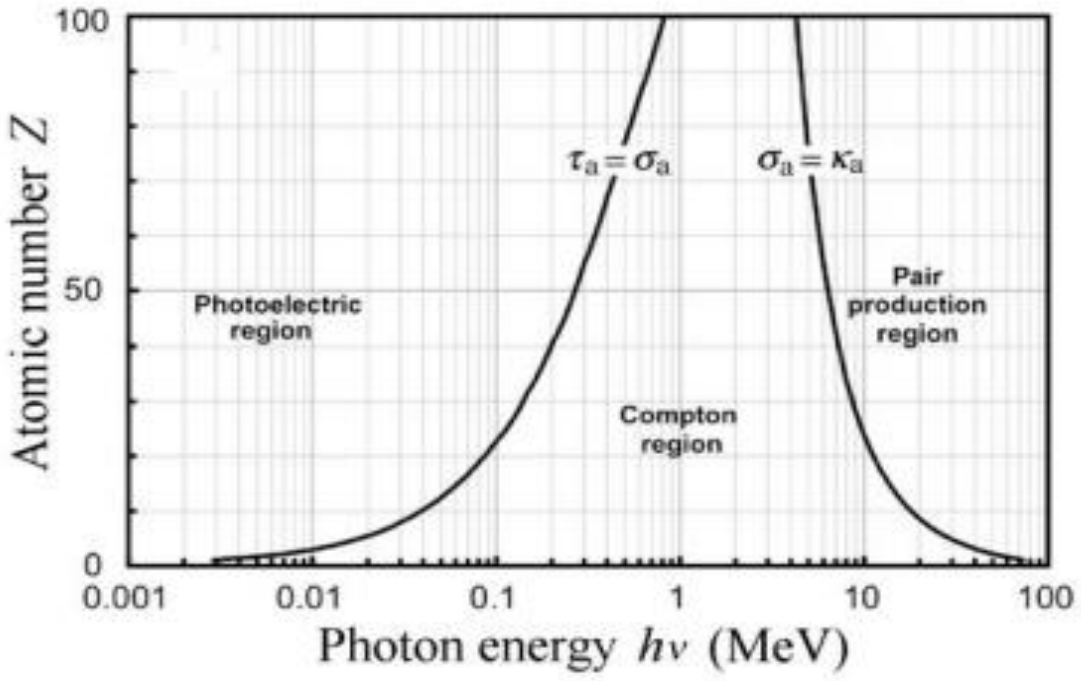

Figure 1: Dominance of photon interaction process (IAEA, 2011)

When photons come into contact with an object they create loose electrons. Matter then slows these electrons down, creating charged pairs. To determine photon energy, photon detectors gauge the amount of charge generated in these pairs (Berekta and Mathew, 1985).

3.7.1 Photoelectric Effect

An atom experiences photoelectric effect when it totally absorbs a photon of gamma radiation, which causes the atom to release one of its electrons. An electron that has been released is called a photoelectron. When a gamma ray photon hits an atom one electron inside it absorbs all the energy. When the electron has more energy than what keeps it attached to the atom it breaks free from its orbit. One can find the energy of the photoelectron by subtracting the binding energy of the electron from the energy of the gamma ray that hits it.

The electron's maximum kinetic energy is determined using equation 3.6.

$$KE_{\max} = h\nu - \phi \tag{3.6}$$

K.E max stands for the highest kinetic energy of the expelled electron, h is Planck's constant, ν is the occurrence rate of gamma rays, ϕ the energy needed to take out an electron from an atom sometimes called the work function. The formula demonstrates that the energy of the emitted electron depends on the work function of the material as well as the energy of the incoming gamma ray.

3.7.2 Compton Effect

A gamma ray photon and an atom's electron interact through a process known as Compton scattering. The gamma ray changes course and loses energy during this process. In the Compton Effect, the Compton wavelength can be utilized to explain the wave-like characteristics of particles, such as gamma rays, in equation 3.7.

$$\Delta\lambda = \frac{h}{mec(1-\cos\theta)} \qquad (3.7)$$

Where $\Delta\lambda$ indicates a shift in the wavelength, h is the Planck's constant, mec is the electron's mass, c is the rate at which light travels and θ is the angle of scattering

Understanding the wave-particle duality of gamma rays relies heavily on the Compton Effect.

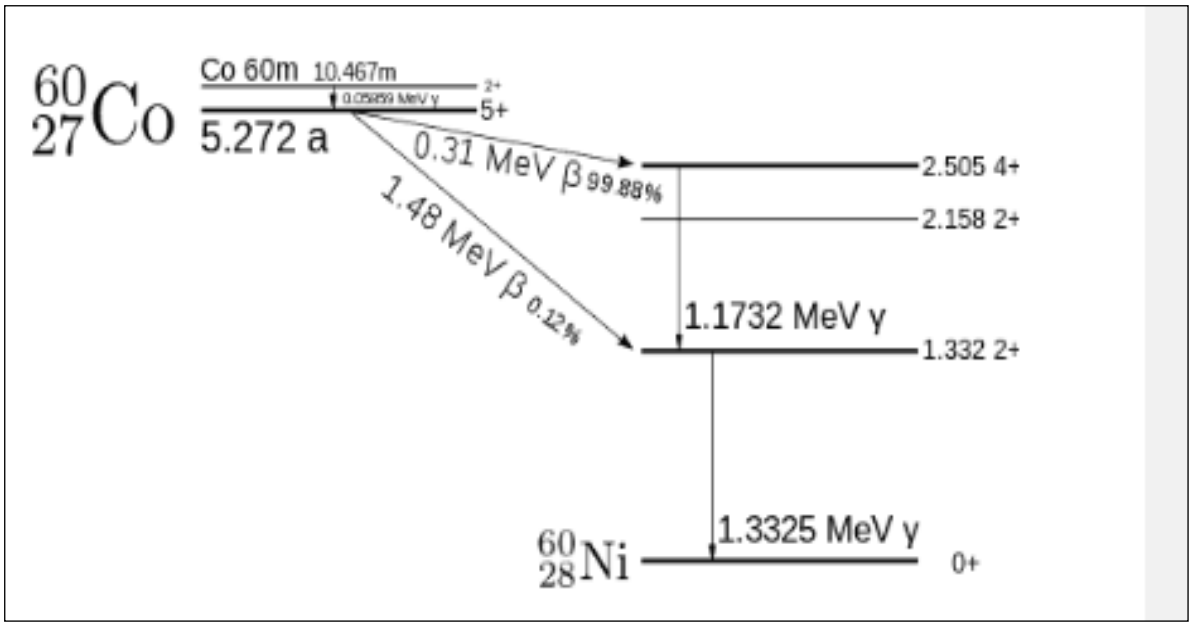

Figure 2: Compton Plateau-Spectrum (IAEA, 2011)

In the collision shown in figure 2, the gamma photon is redirected at an angle theta from its original path.

3.7.3 Pair Production

Pair production takes place when a gamma ray photon possessing energy exceeding 1.022 MeV interacts with the electric field surrounding a nucleus. During this process, the gamma ray transforms into a pair of electron and positron. During pair production, a high-energy gamma ray photon converts its energy into the combined masses of an electron and a positron (its antiparticle) and the particles' kinetic energy. A nucleus is engaged in order to maintain momentum. Pair production is essential for comprehending how high-energy gamma rays behave. Equation 3.8 describes energy conservation in pair production:

$$E_{\lambda} = E_{e-} + E_{e+} + E_{recoil} \tag{3.8}$$

Where E_{γ} is the energy of the incoming gamma ray, E_e is the energy possessed by the electron, E_{e+} is the energy possessed by the positron. and E_{recoil} is the recoil nucleus's energy.

3.8 Human Health and Radiation

Gamma rays influence the environment by impacting ecosystems, air, water, and soil as part of ionizing radiation. For example, Compton scattering may play a role in the ionization of air, water, soil, and living tissues in the environment. Although the environmental doses resulting from Compton scattering are usually minimal, the accumulation of ionization effects has the potential to affect local ecosystems. However, the photoelectric effect causes gamma rays to be

fully absorbed by atoms in the surroundings, leading to ionization of air, water, and biological substances. Ionization has the potential to impact the health of ecosystems, such as plant growth and the welfare of aquatic organisms. Furthermore, pair production can result in the generation of electron-positron pairs and extra gamma rays when high-energy gamma rays interact with atomic nuclei in the surroundings, through positron annihilation. Pair production in high gamma radiation areas can result in higher levels of ionization in the surroundings. This process of ionization has the potential to impact the dynamics of ecosystems, biodiversity, and the overall health of the environment by affecting soil, water, and biological systems.

Gamma rays, a type of ionizing radiation, can impact human health positively or negatively based on factors like dosage, duration of exposure, and specific interaction mechanisms. X-rays are widely utilized in medical diagnosis (e.g., X-ray imaging) and cancer treatment through radiation therapy (Procz *et al*., 2019). Regulated gamma ray exposure aids in precise disease diagnosis and focused cancer therapy. Nevertheless, these rays have the potential to harm tissues. When living tissue is exposed to gamma rays, atoms and molecules can become ionized, causing harm to cells. This harm could interfere with typical cell functions and potentially lead to genetic changes, raising the likelihood of developing cancer.

Exactly, the process of Compton scattering causes gamma rays to lose energy and can ionize atoms in biological tissues. This ionization has the potential to harm biomolecules such as DNA, increasing the likelihood of mutations and the risk of cancer. In addition to Compton scattering, Photoelectric effect is another process in which gamma rays are fully absorbed, leading to the

emission of electrons. This procedure has the ability to transfer a large amount of energy to a small area of tissue, which can result in specific injury. Alternatively, pair production can result in the generation of electron-positron pairs within the tissue. The following destruction of these particles results in more gamma rays being released, aiding in the ionization and possible harm to nearby tissue.

CHAPTER FOUR

MATERIALS AND METHODS

4.1 Sampling and Sample Preparation

Kangundo road starts at Outering road and stretches all the way into the Machakos County. Situated in the east of Nairobi County Kenya spanning roughly 67 kilometers in length. The research area is about 1480 meters above sea level and crosses different latitudes 1^0 2" South, longitude 36^0 66" East. The materials utilized in the construction of infrastructure along this route consist of sand, clay brick, and concrete block. Building material sold or used along Kangundo Road many comes from surrounding Counties such as Kitui (UN-HABITAT, 2009). The existence of granite and phosphate deposits in Machakos County and the surrounding area has resulted in elevated radiation levels. According to Achola (2009), the rocks in the area that contain granite and phosphate amplify the presence of Natural Radiation Sources (NRS). Heavy rainfall in these areas erodes native rocks, releasing radioactive traces that settle in riverbanks and eventually serve as resources for sand mining and, eventually, sand collection for construction needs in neighboring counties like Nairobi (Okalebo et al., 2009).

According to UNSCEAR (2000) building materials emit around 0. 008 micro-Sieverts (μSv) every hour. The findings of this research will give important information for future use by giving data and statistics on the number of radionuclides and the level of radiation hazards in the area being studied.

Kangundo Road was selected due its significant growth in construction projects and high population density. In order to guarantee a representative sample, a purposive random sampling method was utilized. This boosted the statistical sensitivity of the gathered data hence validating our results. Thirty samples were collected from various construction sites within the study area i.e. 14 clay samples, 9 brick samples, and 7 concrete blocks samples, with a distance difference of 1 kilometer between collection points. These construction materials were chosen for analysis because they are frequently used in the area for building purposes. Every sample was meticulously gathered, with a weight ranging from 0.5 Kg to 1 Kg, and GPS coordinates were noted for accurate location determination.

The samples were then processed by grinding into fine powder, followed by sieving through a 1 x 1 mm mesh screen to achieve consistent particle sizes. Subsequently, they were dried in an oven at 110 °C for a minimum of 12 hours prior to examination. This standardized procedure guarantees that each sample is in a uniform condition, facilitating precise analysis. The dehydrated samples are placed into airtight containers and correctly identified to avoid any potential contamination or mix up while during analysis. After this, the specimens were stored for 4 weeks. This was to cater for the establishment of radioactive decay balance and secular equilibrium within the uranium (^{238}U) and thorium (^{232}Th) isotopes and their progenies.

4.2 NaI (T1) Gamma-Ray Spectrometer

In order to measure radiation levels in building materials, a 76 × 76 mm sodium iodide thallium (NaI(Tl) gamma-ray detector was used as seen in figure 3. The selection of the detector was made due to its demonstrated efficiency in precisely detecting gamma radiation. The Multichannel analyser (MCA) then collected and recorded the pulse of charge representing the energy of the incoming gamma photons which was subsequently showcased as a spectrum on a monitor.

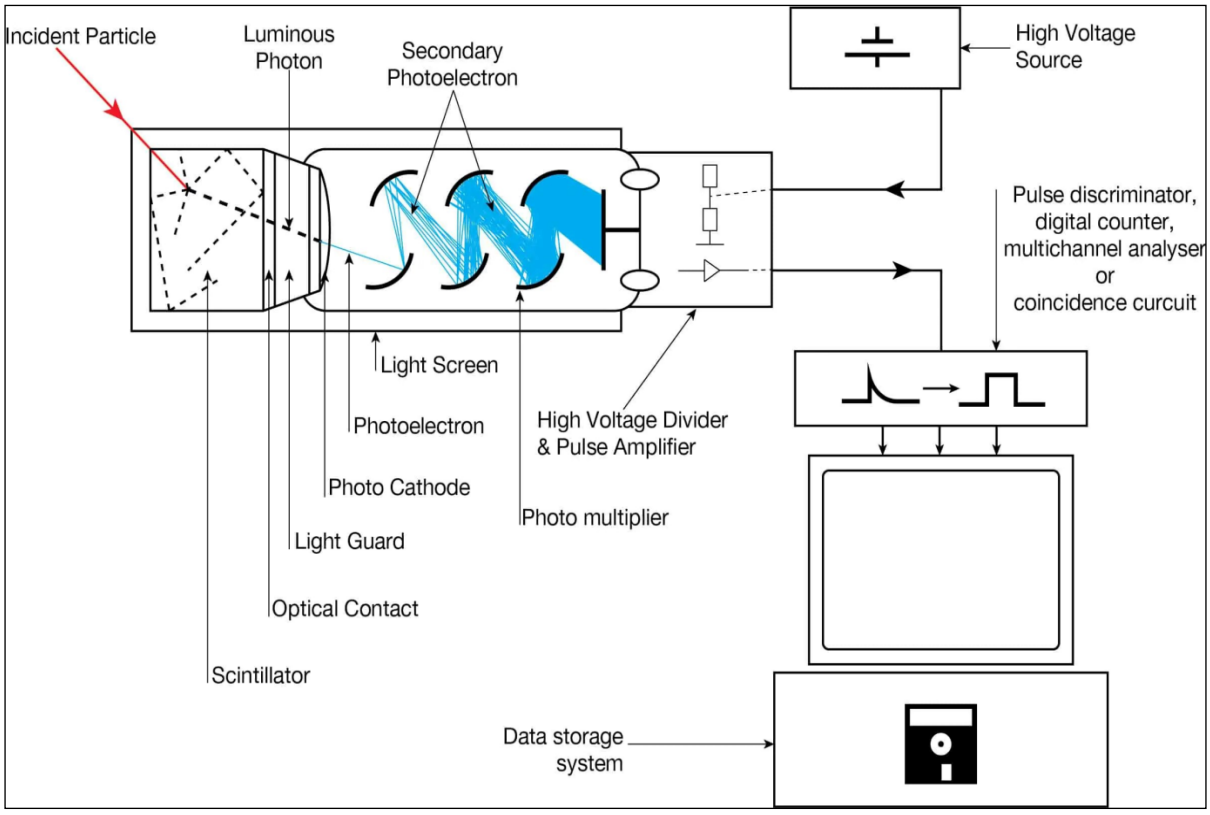

Figure 3: Gamma-ray spectrometry using NaI(Tl) detector (IAEA, 2011).

4.2.1 Calibration in NaI(T1) Spectrometry

Analyzing the building material samples is an essential component of this study. The objective was to precisely gauge the amounts of gamma-ray emissions from radionuclides found in the construction materials. To accomplish this, the process of identifying regions of interest (ROIs) within the gamma-ray spectra was carried out. The attention in the spectra was directed towards areas that match the energy levels of the established photopeaks of certain radionuclides. More precisely, the focus was on the photopeaks located around 1460 keV (from potassium^{-40} or ^{40}K), 1765 keV (from bismuth-214 or ^{214}Bi), and 2615 keV (from thallium-208 or ^{208}TI). These regions of interest (ROIs) are essential for evaluating radionuclide levels, as each peak represents a particular radionuclide. A duration of 30,000 seconds was scheduled for each sample on the calibrated NaI(Tl) spectrometer. The spectrum obtained was saved as text files for future examination.

The highest points were then utilized to infer the relationship between Energy and Channel. Using second order polynomial in the form of Equation (4.1), the photon energy is represented as a function of channel number (Ibrahim and Awadallah, 2009)

$$E = Y_0 + C_1 + C_2 B^2 \qquad (4.1)$$

Channel number is represented by B, with constants Y_0, C_1, and C_2 having fitted values of 13.867 ± 0.693, 3.513 ± 0.176, and 0.0011 ± 0.0001 as shown in Table 1.

The graph presented in figure 4.2 illustrates the energy calibration graph along with the parameters employed. Thus, using the least square fitting of the calibration, a polynomial was generated, where E stands for photon energy and B for the channel number.

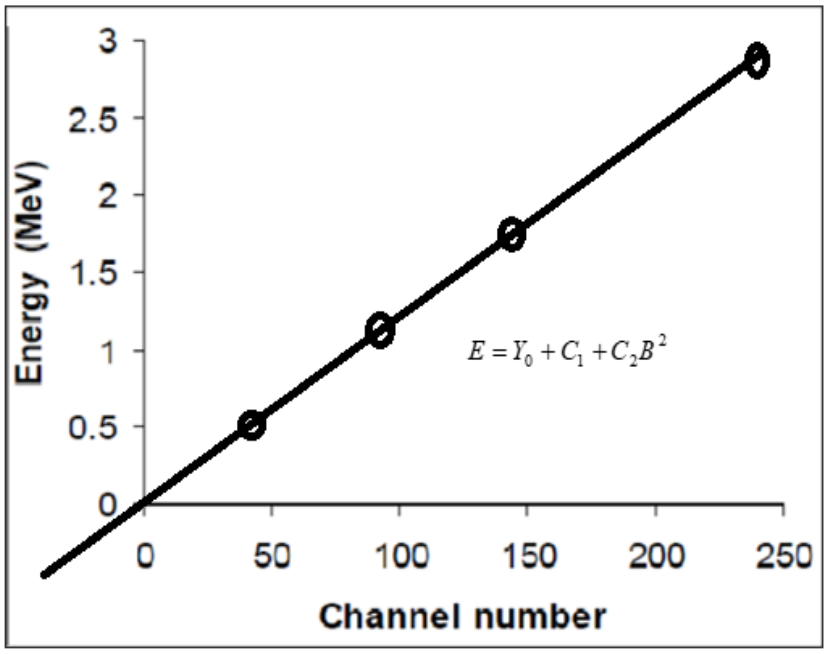

Figure 3: Energy-channel calibration curve for the NaI(Tl) detector

Table 1: The polynomial regression for the energy calibration of NaI(Tl) detector

Constant	Fitted value
Y_0	13.867±0.693
C_2	0.0011±0.0001
C_1	3.513±0.176

4.2.2 Measurement of Background Radiation.

A similar plastic vessel holding approximately 400 ± 10 g of distilled water was utilized to assess background radiation levels. Measurement of background radiation was done for a duration of 30,000 seconds, and the result subtracted from the recorded spectrum of all the building material samples analyzed in the study.

Water contains large number of ions, mostly originating from the soil including sodium, calcium, iron, copper sulfates, carbonates, and nitrates. Deionized water is defined as having no ions hence any counts it records during the experiment are likely due to the ambient surroundings of the detector.

4.2.3 NaI(Tl) Detector Energy Resolution

Energy resolution refers to a detector's capability to differentiate between two photo peaks that are in close proximity to each other. Detector energy resolution can be represented in form of full width at half maximum (FWHM), as outlined in equation (4.2) (Khandoker, 2015). Plate 1 indicates how the determination was achieved by applying the Gaussian fitting method to fit the photo peak of Cs-137 by using Equation (4.3)

$$\text{Energy resolution} = \frac{\text{FWHM}}{\text{E}} \times 100\% \qquad (4.2)$$

$$y = y_0 + \frac{A}{w\sqrt{\frac{\pi}{2}}} e^{\frac{(x-x_c)^2}{w^2}} \qquad (4.3)$$

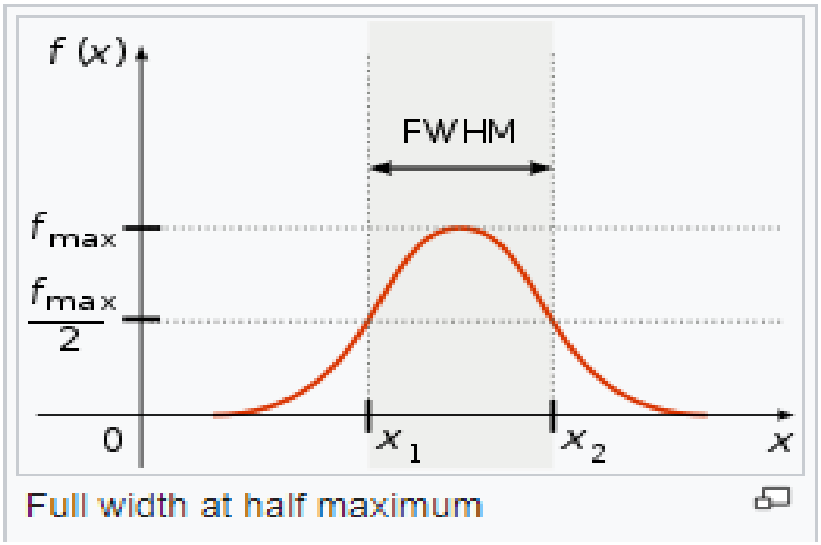

Figure 5: Full energy peak for 137-Cs measured in this work

The spectrum curve sample for building material, Sample K1, is depicted in figure 5

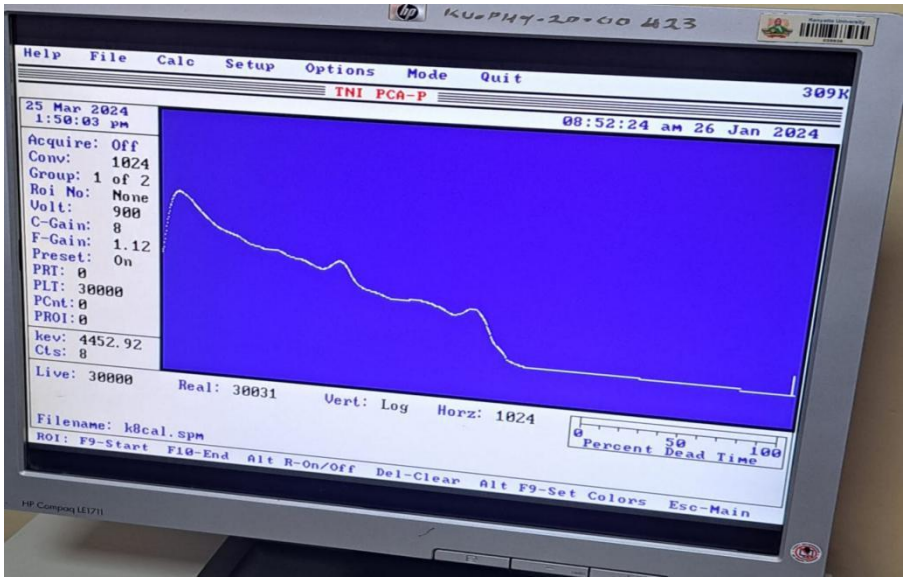

Figure 6: Screenshot of the Gamma ray spectrum for one of sand samples.

4.2.4 Detector Efficiency

Detector efficiency is the likelihood that a gamma ray once discharged will interact with the detector crystal and create a specific count. The twinkling process is the foundation for the NaI(TI) detector's operation. NaI(TI) detectors do not have long delays like semiconductor gamma ray detectors. Due to the detector's 0.01% dead time, a very high detection efficiency was achieved when the gamma source was positioned directly above it, leaving zero centimeters between the sample and the detector. This was verified by checking the detector's active and inactive times after each counting session.

Consequently, the utilization of the gamma detector significantly decreased the likelihood of overlooking an emitted photon. Equation (4.4) was used to calculate the efficiency of the standard radionuclides in this study.

$$\mu = \frac{N}{(A \times T \times \rho \times M)} \tag{4.4}$$

N stands for the total count rate *T* is the counting time, ρ is the radionuclide's emission probability, *M* is the mass of the sample and *A* is the Activity.

Table 2: Detectors' efficiency and intensity for the standard radionuclides used in this work. Nurgül *et al* (2024)

Nuclide	Energy (KeV)	Intensity	Emission probability	Mass (Kg)	Efficiency	Activity (Bq/Kg)
^{232}Th	238	26.4667	0.4316	0.4	0.079951	1932
^{238}U	351	19.5907	0.3534	0.4	0.046952	2950
^{40}K	1460	8.757	0.1066	0.4	0.021031	9262

Different types of radiation (alpha, beta, gamma, neutrons) interact with detectors in different ways. For example, alpha particles are easily absorbed and therefore require detectors with high sensitivity to surface interactions, while gamma rays require materials with high Z-values for better absorption. This was the reason the detector efficiency was different for different NORMs.

4.3 Samples Analysis

The main goal was to accurately measure the gamma-ray activity levels present in these materials. To accomplish this, ROIs in the gamma-ray spectra were identified as shown in figure (6). The spectra centered on areas that matched the energy levels of established photopeaks for certain radionuclides. In particular, the photopeaks located around 1460 keV (from ^{40}K), 1765 keV (from ^{214}Bi), and 2615 keV (from ^{208}TI). These regions of interest are essential for evaluating radionuclide levels, as each peak represents a distinct radionuclide. For every sample, a time of 30,000 seconds was allocated for counting by the calibrated NaI(Tl) spectrometer. The obtained spectra were saved as text files for future analysis.

The process for sample analysis proceeded as follows;

i. Using a calibrated Na(Tl) spectrometer, each sample was analyzed for thirty thousand seconds. The spectrum of each sample was then saved in text files on a PC based Multichannel Analyzer (MCA).

ii. The net counts were obtained by deducting the background count from each sample count

iii. The Activity concentration in all samples was then determined as shown in (4.4).

Figure 7: A screenshot of regions of interest in the spectrum taken for one of the samples

4.4 Radioactivity Concentration Levels

The equation 4.5 (Beretka J., Mathew P. J.,1985) was utilized to calculate each radionuclide's activity concentration (*A*) in $Bqkg^{-1}$.

$$A = \frac{N}{\varepsilon \times T \times I \times M} \tag{4.5}$$

The values of *A, N, ε, T, I* and *M* represents the activity concentration measured in $BqKg^{-1}$, the net peak area (N) obtained following the subtraction of background for the γ-ray line at energy E, the detector efficiency (ε), the gamma intensity (I) associated with the specific photopeak, and the mass of the sample (kg).This calculation enables precise quantification of radionuclide concentrations in building materials, which is crucial for evaluating possible health and environmental hazards. The results are displayed inform of a bar graph as shown in figure (7).

4.5 Calculations of the Radiological Parameters

4.5.1 Calculation Absorbed Dose Rate

The absorbed dose rate was calculated using Equations 4.6 and 4.7 for clay bricks and sand, in accordance with the guidelines established in the 1988 UNSCEAR report.

For clay bricks:

$$D = 0.92 \times A_U + 1.1 \times A_{Th} + 0.08 \times A_K \tag{4.6}$$

For Sand

$$D = 0.43 \times A_U + 0.666 \times A_{Th} + 0.042 \times A_K \quad (4.7)$$

In the formulars, *D* represents the absorbed dose rate measured in nanograys per hour (nGy/h). A_U denotes the activity concentration of uranium-238 (^{238}U) expressed in Bq/Kg, A_{Th} indicates the activity concentration of thorium-232 (^{232}Th) also in Bq/Kg, and A_K signifies the activity concentration of potassium-40 (^{40}K) in Bq/Kg found within the samples.Calculations of the dose rate is crucial in determining the possible radiation exposure for individuals residing close to buildings constructed from these materials. The results are displayed inform of a bar graph as shown in figure (9).

4.5.2 Annual Effective Dose Rate (AEDR)

The AEDR was determined by applying the formula: (UNSCEAR, 2008)

$$AEDR = D \times T \times F \quad (4.8)$$

where *D* is the absorbed dose rate in $nGyh^{-1}$ is determined, *T* refers to the amount of time spent outdoors (measured in hours per year). In our situation, the calculation was done as 3500 hours per year (40%) and *F* is the conversion factor with a numerical value of 0.7×10^{-6} $SvGy^{-1}$.

This analysis gives us information about the possible health impacts in future on people who are in contact with radiation from the construction materials. The results are displayed inform of a bar graph as shown in figure (10).

4.5.3 Radium Equivalent Activity

The radium equivalent activity was calculated using equation (4.9) (Flores *et al.*, 2005).

$$Ra_{eq} = A_U + 1.43 \times A_{Th} + 0.077 \times A_K \quad (4.9)$$

In the equation, A_U the concentration level of uranium in the activity (^{238}U) in $Bqkg^{-1}$,A_{Th} is the thorium concentration in the activity (^{232}Th) in $Bqkg^{-1}$ and A_K is the potassium (^{40}K) activity concentration in $Bqkg^{-1}$ within the construction materials. The radium equivalent activity provides a simple way to evaluate radiation dangers and is a crucial measurement for ensuring safety standards are met. The results are displayed inform of a bar graph as shown in figure (8).

4.5.4 Hazard Index Hex

1. The annual contribution of naturally occurring radionuclides to the gamma dose is used to determine the hazard index.

In connection with the additional gamma radiation that leads to an annual effective dose increase of up to 0.3 mSv/y for the general population, the bulk limits for radionuclides ^{238}U, ^{232}Th, and ^{40}K are established at 370 Bq/kg, 279 Bq/kg, and 4810 Bq/kg respectively (Mann and Gartinkil, 1966). The calculation of Hazard Index was done using equation (4.10) (Beretka and Mathew, 1985).

$$H_{ex} = \frac{A_U}{370} + \frac{A_{Th}}{259} + \frac{A_K}{4810} \quad (4.10)$$

where A_U, A_{Th}, and A_K depict the levels of activity concentrations in Bq/kg for Uranium^{-238} (^{238}U), thorium^{-232} (^{232}Th), and potassium^{-40} (^{40}K) in the building materials respectively.

The hazard index is a useful tool for evaluating the safety and suitability of construction materials in relation to radiation levels. The results are displayed inform of a bar graph as shown in figure (11).

4.6 Quality Control

To achieve research results that are consistent, dependable, and backed by evidence, the following steps were carried out.

a) The materials from a specific location were correctly identified to prevent sample mix-up during analysis.

b) In order to prevent contamination during transport to Kenyatta University laboratory, the samples were safely kept in sealed containers.

c) The distribution of the area covered was made uniform to enhance the statistical representation of the sample.

d) Precautions were taken to handle tools carefully during sample collection and storage to avoid any contamination that could affect the results.

e) The region of interest (ROI) was consistently chosen for each spectrum during the intensity determination process.

f) NaI(T1) the detector was calibrated using standard samples from IAEA before a subsequent sample was analysed.

CHAPTER FIVE

RESULTS AND DISCUSSION

5.1 Radioactivity Concentration

The research evaluated the levels of radioactivity concentration for natural radionuclides and radiological hazards from building materials used along Kangundo road in Nairobi City County. For this research, the NaI(Tl) detector proved to be very helpful. Radiological parameters were evaluated based on radioactivity concentration, which was determined after activity concentrations in samples of building materials were determined. Various parameters like radium equivalent, absorbed dose rate, annual effective dose rate and hazard index (External) were calculated from which the results were presented in form of tables and bar graphs.

5.1.1 Radioactivity Concentration of Building Materials from Kangundo Road

The materials for building in Kangundo Road come from counties near Nairobi County. According to UN-HABITAT (2009), Machakos, Kitui, Narok and Kajiado Counties are the major sources of building materials found on Kangundo road. Granite and phosphate rock formations in these Counties, which experience weathering due to changing weather patterns, contributes to the creation of sand in the region with increased amounts of radioactive substances (Rotich, 2015). Variations in climate also lead to the erosion of rocks, resulting in the accumulation of radionuclide remnants in river banks which are later used in construction when mixed with sand. Furthermore, the eroded particles create topsoil that is used to make clay bricks.

The measured radioactive concentration levels for radionuclides ^{40}K, ^{238}U, were calculated using equation (4.5) and displayed in Table 3. The average radioactivity concentration of radionuclide ^{40}K exceeded that of ^{238}U and ^{232}Th because the primary source of naturally occurring radionuclides is the potassium. The detected levels of radioactivity for ^{40}K ranged from 118 ± 6 $Bqkg^{-1}$ to 2392 ± 120 $Bqkg^{-1}$, resulting in an average of 860 ± 40 $Bqkg^{-1}$. The concentration levels for ^{238}U ranged from 24 ± 1 Bq/kg to 410 ± 20 Bq/kg, resulting in an average of 78 ± 4 Bq/kg. For ^{232}Th, the levels varied from 55 ± 3 Bq/kg to 610 ± 30 Bq/kg, with an average of 160 ± 10 Bq/kg.

Table 3: Activity concentration levels for the natural radionuclides ^{40}K, ^{238}U and ^{232}Th of building materials sampled in this work.

SAMPLE SITE	LATITUDES	LONGITUDES	^{238}U Bq/kg	^{40}K Bq/kg	^{232}Th Bq/kg	SAMPLE TYPE	SAMPLE ORIGIN
K1	36^0,65.1972’	01^0 ,10.758’	291 ± 2	391 ± 2	136 ± 7	SAND	EMBU
K2	36^0,17.655’	01^0 ,55.324’	315 ± 2	603 ± 3	163 ± 8	SAND	MACHAKOS
K3	36^0,57.677’	01^0 ,20.963’	412 ± 2	744 ± 4	612 ± 3	SAND	KITUI
K4	36^0,57.00’	01^0 ,20.963’	291 ± 2	2082 ± 1	95 ± 5	CONCRETE	KAJIADO
K5	36^0,54.390’	01^0 ,15.351’	34 ± 2	118 ± 6	163 ± 9	CONCRETE	MULOLONGO
K6	36^0,57.343’	01^0 ,16.890’	29 ± 1	1060 ± 5	211 ± 1	SAND	KITUI
K7	36^0,55.369’	01^0 ,15.437’	29 ± 1	1554 ± 8	163 ± 8	CONCRETE	MULOLONGO
K8	36^0,55.00’	01^0 ,15.430’	52 ± 3	1724 ± 9	150 ± 7	CONCRETE	MULOLONGO
K9	36^0,38.913’	01^0 ,15.751’	27 ± 1	2392 ± 1	136 ± 7	SAND	MAI MAHIU
K10	36^0,58.606’	01^0 ,15.367’	32 ± 2	904 ± 5	245 ± 1	SAND	NAROK
K11	36^0,59.517’	01^0 ,13.192’	36 ± 2	1690 ± 8	150 ± 7	BRICK	KAJIADO
K12	36^0,00.370’	01^0 ,16.854’	99 ± 5	297 ± 2	116 ± 6	SAND	MAI MAHIU
K13	36^0,58.940’	01^0 ,14.765’	36 ± 2	527 ± 3	204 ± 1	SAND	KITUI
K14	36^0,58.827’	01^0 ,15.706’	32 ± 2	1771 ± 9	102 ± 5	SAND	MACHAKOS
K15	36^0,59.215’	01^0 ,15.885’	24 ± 1	339 ± 2	163 ± 8	SAND	NJIRU

K16	36^0,58.2531’	01^0 ,18.465’	39 ± 2	904 ± 5	197 ± 1	CONCRETE	KAJIADO
K17	37^0,01.565’	01^0 ,14.349’	36 ± 2	297 ± 2	116 ± 6	SAND	MAI MAHIU
K18	37^0,00.566’	01^0 ,16.833’	34 ± 2	344 ± 2	55 ± 3	SAND	MWALA
K19	37^0,01.291’	01^0 ,16.553’	34 ± 2	353 ± 2	116 ± 6	SAND	MASINGA
K20	37^0,02.206’	01^0 ,16.992’	44 ± 2	396 ± 2	211 ± 1	SAND	KATANI
K21	37^0,02.890’	01^0 ,17.064’	42 ± 2	1813 ± 9	211 ± 1	CONCRETE	THIKA
K22	37^0,03.484’	01^0 ,17.168’	34 ± 2	471 ± 2	82 ± 4	CONCRETE	LONDIANI
K23	37^0,03.919’	01^0 ,17.256’	49 ± 3	151 ± 8	109 ± 5	BRICK	LONDIANI
K24	37^0,04.146’	01^0 ,16.917’	56 ± 3	772 ± 4	61 ± 3	BRICK	LONDIANI
K25	37^0,04.612’	01^0 ,16.937’	44 ± 2	509 ± 3	177 ± 9	BRICK	MULOLONGO
K26	37^0,06.364’	01^0 ,17.115’	49 ± 2	932. ± 5	82 ± 4	BRICK	THIKA
K27	37^0,06.898’	01^0 ,17.088’	41 ± 2	857 ± 4	102 ± 5	BRICK	RUIRU
K28	37^0,07.088’	01^0 ,17.161’	32 ± 2	556 ± 3	122 ± 6	BRICK	THIKA
K29	37^0,07.327’	01^0 ,16.564’	36 ± 2	551 ± 3	190 ± 1	BRICK	MACHAKOS
K30	37^0,08.307’	01^0 ,16.638’	36 ± 2	692 ± 3	156 ± 8	BRICK	RUIRU

Table 4: The mean activity concentration of radionuclide in building materials compared to the world average values.

Radionuclide	Study area mean values ($Bqkg^{-1}$)	WORLD AVERAGE ($Bqkg^{-1}$) (UNSCEAR,2000)
^{40}K	859.7 ± 43	420
^{238}U	78.1 ± 4	33
^{232}Th	159.7 ± 8	45

Figure 8 illustrates the distribution of activity for ^{238}U, ^{232}Th, and ^{40}K at the sampling locations along Kangundo Road. From table 3 and figure 8, the regions with samples labelled K4, K8, K9, K14 and K21 had the highest concentrations of radioactivity for ^{40}K while K3 had the highest concentration for ^{238}U and ^{232}Th. The levels of radioactivity from ^{40}K were elevated in all samples analyzed when compared to other radionuclides, the activity concentrations of ^{238}U exceeded the global average of 33 Bq/kg in some samples taken from Kangundo road. Similarly, the levels of radioactivity concentration in ^{232}Th were elevated in the majority of these samples, surpassing the global average of 45 Bq/kg (UNSCEAR, 2000). The significant radioactivity levels in most samples collected along Kangundo road were attributed to their source, such as Kitui, which contains high concentrations of igneous rocks.

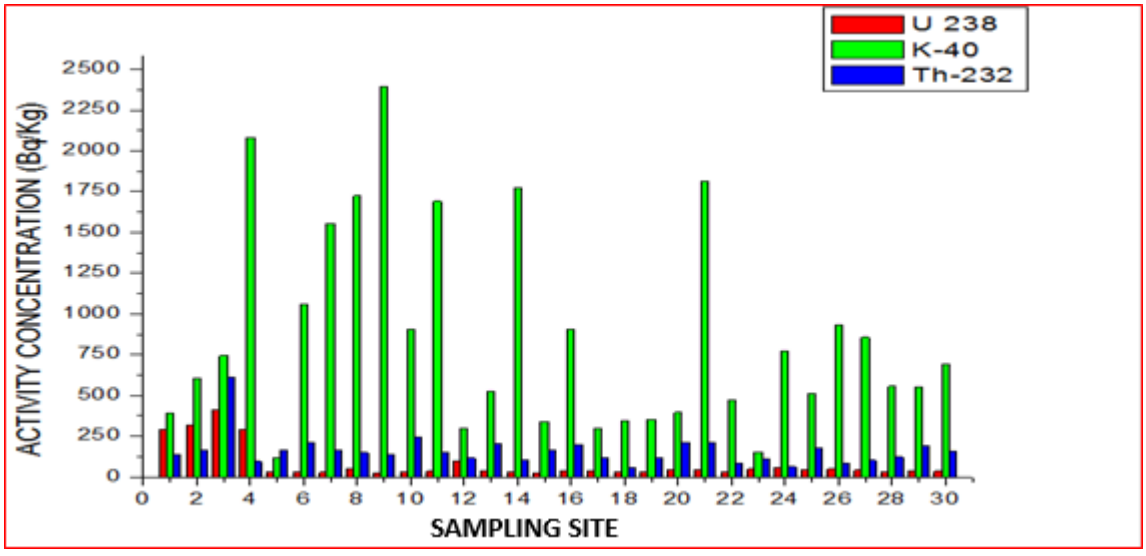

Figure 8: Concentration levels of ^{238}U, ^{232}Th and ^{40}K in the samples

5.1.2 Radium Equivalent of Building Materials

Thirty randomly selected samples were collected along the Kangundo Road. and radium equivalent for each sample was determined using Equation (4.9).

Table 5: Radium equivalent of Building Materials along Kangundo road

SAMPLE SITE	LATITUDES	LONGITUDES	Raeq (Bq/Kg)	SAMPLE TYPE	SAMPLE ORIGIN
K1	36^0,65.1972’	01^0 ,10.758’	515.33 ± 26	SAND	EMBU
K2	36^0,17.655’	01^0 ,55.324’	594.65 ± 30	SAND	MACHAKOS
K3	36^0,57.677’	01^0 ,20.963’	1343.9 ± 7	SAND	KITUI
K4	36^0,57.00’	01^0 ,20.963’	587.11 ± 29	CONCRETE	KAJIADO
K5	36^0,54.390’	01^0 ,15.351’	386.80 ± 19	CONCRETE	MULOLONGO
K6	36^0,57.343’	01^0 ,16.890’	381.91 ± 19	SAND	KITUI
K7	36^0,55.369’	01^0 ,15.437’	411.99 ± 20	CONCRETE	MULOLONGO
K8	36^0,55.00’	01^0 ,15.430’	397.40 ± 20	CONCRETE	MULOLONGO
K9	36^0,38.913’	01^0 ,15.751’	405.24 ± 20	SAND	MAI MAHIU
K10	36^0,58.606’	01^0 ,15.367’	422.69 ± 21	SAND	NAROK
K11	36^0,59.517’	01^0 ,13.192’	380.22 ± 19	BRICK	KAJIADO
K12	36^0,00.370’	01^0 ,16.854’	286.91 ± 14	SAND	MAI MAHIU
K13	36^0,58.940’	01^0 ,14.765’	368.49 ± 18	SAND	KITUI
K14	36^0,58.827’	01^0 ,15.706’	313.56 ± 16	SAND	MACHAKOS
K15	36^0,59.215’	01^0 ,15.885’	283.57 ± 14	SAND	NJIRU
K16	36^0,58.2531’	01^0 ,18.465’	390.27 ± 20	CONCRETE	KAJIADO
K17	37^0,01.565’	01^0 ,14.349’	224.35 ± 11	SAND	MAI MAHIU
K18	37^0,00.566’	01^0 ,16.833’	138.18 ± 70	SAND	MWALA
K19	37^0,01.291’	01^0 ,16.553’	226.28 ± 11	SAND	MASINGA
K20	37^0,02.206’	01^0 ,16.992’	325.36 ± 16	SAND	KATANI
K21	37^0,02.890’	01^0 ,17.064’	484.50 ± 24	CONCRETE	THIKA
K22	37^0,03.484’	01^0 ,17.168’	186.85 ± 90	CONCRETE	LONDIANI
K23	37^0,03.919’	01^0 ,17.256’	215.69 ± 11	BRICK	LONDIANI

K24	37^0,04.146’	01^0 ,16.917’	202.68 ± 10	BRICK	LONDIANI
K25	37^0,04.612’	01^0 ,16.937’	335.44 ± 17	BRICK	MULOLONGO
K26	37^0,06.364’	01^0 ,17.115’	236.94 ± 12	BRICK	THIKA
K27	37^0,06.898’	01^0 ,17.088’	252.91 ±1 3	BRICK	RUIRU
K28	37^0,07.088’	01^0 ,17.161’	249.18 ± 12	BRICK	THIKA
K29	37^0,07.327’	01^0 ,16.564’	350.85 ± 18	BRICK	MACHAKOS
K30	37^0,08.307’	01^0 ,16.638’	313.12 ± 16	BRICK	RUIRU

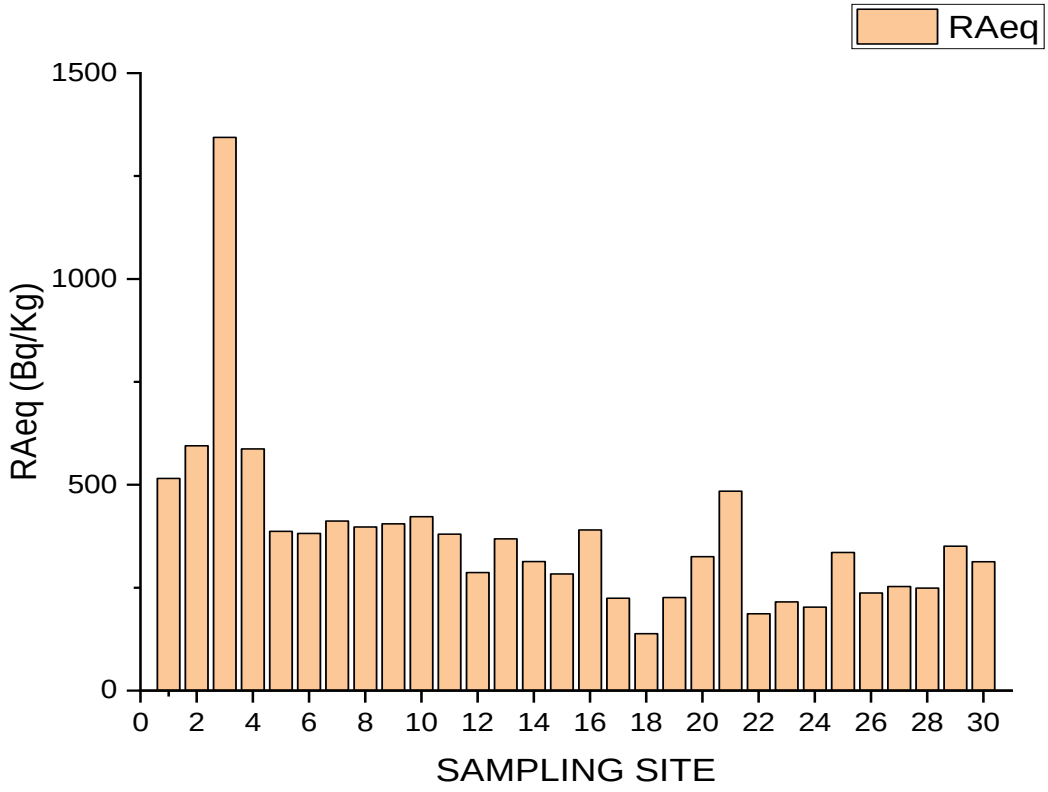

Figure 9: Radium equivalent for the building materials

Radium Equivalent values recorded ranged between 138 ± 7 Bq/Kg and 1344 ± 67 Bq/Kg, with samples K1, K2, K3, K4, and K21 exceeding the globally recommended safety threshold of 370 $Bqkg^{-1.}$

5.2 Dose Rate

The dose rate for sand and clay bricks was assessed based on randomly selected sample sites using equations (4.6) and (4.7). The absorbed dose rate ranged from 65 ± 3 to 616 ± 31 $nGyh^{-1}$, which remains below the international safety threshold of 1500 $nGyh^{-1}$. The results indicated that the dose rate exceeded the global average of 54 $nGyh^{-1}$, but remained within the acceptable global safety limit of 1500$nGyh^{-1}$ (UNSCEAR, 2000). The results of the dose rate analysis were presented in Table 6 and illustrated graphically in Figure 10.

Table 6: The dose rate for sample collected along Kangundo road

Sampling site	Latitude	Longitude	Dose rate (nGy/h)	Sample type	Sample Origin
K1	36^0,65.1972’	01^0 ,10.758’	231.97 ± 10	SAND	EMBU
K2	36^0,17.655’	01^0 ,55.324’	269.39 ± 13	SAND	MACHAKOS
K3	36^0,57.677’	01^0 ,20.963’	615.76 ± 31	SAND	KITUI
K4	36^0,57.00’	01^0 ,20.963’	272.83 ± 14	CONCRETE	KAJIADO
K5	36^0,54.390’	01^0 ,15.351’	128.15 ± 60	CONCRETE	MULOLONGO
K6	36^0,57.343’	01^0 ,16.890’	197.34 ± 10	SAND	KITUI
K7	36^0,55.369’	01^0 ,15.437’	186.37 ± 90	CONCRETE	MULOLONGO
K8	36^0,55.00’	01^0 ,15.430’	193.84 ± 10	CONCRETE	MULOLONGO
K9	36^0,38.913’	01^0 ,15.751’	202.47 ± 10	SAND	MAI MAHIU
K10	36^0,58.606’	01^0 ,15.367’	556.28 ± 28	SAND	NAROK
K11	36^0,59.517’	01^0 ,13.192’	186.16 ± 90	BRICK	KAJIADO

K12	36^0,00.370’	01^0 ,16.854’	131.91 ± 70	SAND	MAI MAHIU
K13	36^0,58.940’	01^0 ,14.765’	173.56 ± 90	SAND	KITUI
K14	36^0,58.827’	01^0 ,15.706’	155.78 ± 80	SAND	MACHAKOS
K15	36^0,59.215’	01^0 ,15.885’	133.28 ± 70	SAND	NJIRU
K16	36^0,58.2531’	01^0 ,18.465’	185.92 ± 90	CONCRETE	KAJIADO
K17	37^0,01.565’	01^0 ,14.349’	105.01 ± 50	SAND	MAI MAHIU
K18	37^0,00.566’	01^0 ,16.833’	65.26 ± 30	SAND	MWALA
K19	37^0,01.291’	01^0 ,16.553’	106.34 ± 50	SAND	MASINGA
K20	37^0,02.206’	01^0 ,16.992’	175.69 ± 90	SAND	KATANI
K21	37^0,02.890’	01^0 ,17.064’	235.22 ± 12	CONCRETE	THIKA
K22	37^0,03.484’	01^0 ,17.168’	88.70 ± 40	CONCRETE	LONDIANI
K23	37^0,03.919’	01^0 ,17.256’	176.36 ± 50	BRICK	LONDIANI
K24	37^0,04.146’	01^0 ,16.917’	180.35 ± 50	BRICK	LONDIANI
K25	37^0,04.612’	01^0 ,16.937’	275.17 ± 80	BRICK	MULOLONGO
K26	37^0,06.364’	01^0 ,17.115’	208.94 ± 60	BRICK	THIKA
K27	37^0,06.898’	01^0 ,17.088’	218.56 ± 60	BRICK	RUIRU
K28	37^0,07.088’	01^0 ,17.161’	207.97 ± 60	BRICK	THIKA
K29	37^0,07.327’	01^0 ,16.564’	286.80 ± 80	BRICK	MACHAKOS
K30	37^0,08.307’	01^0 ,16.638’	260.71 ± 70	BRICK	RUIRU

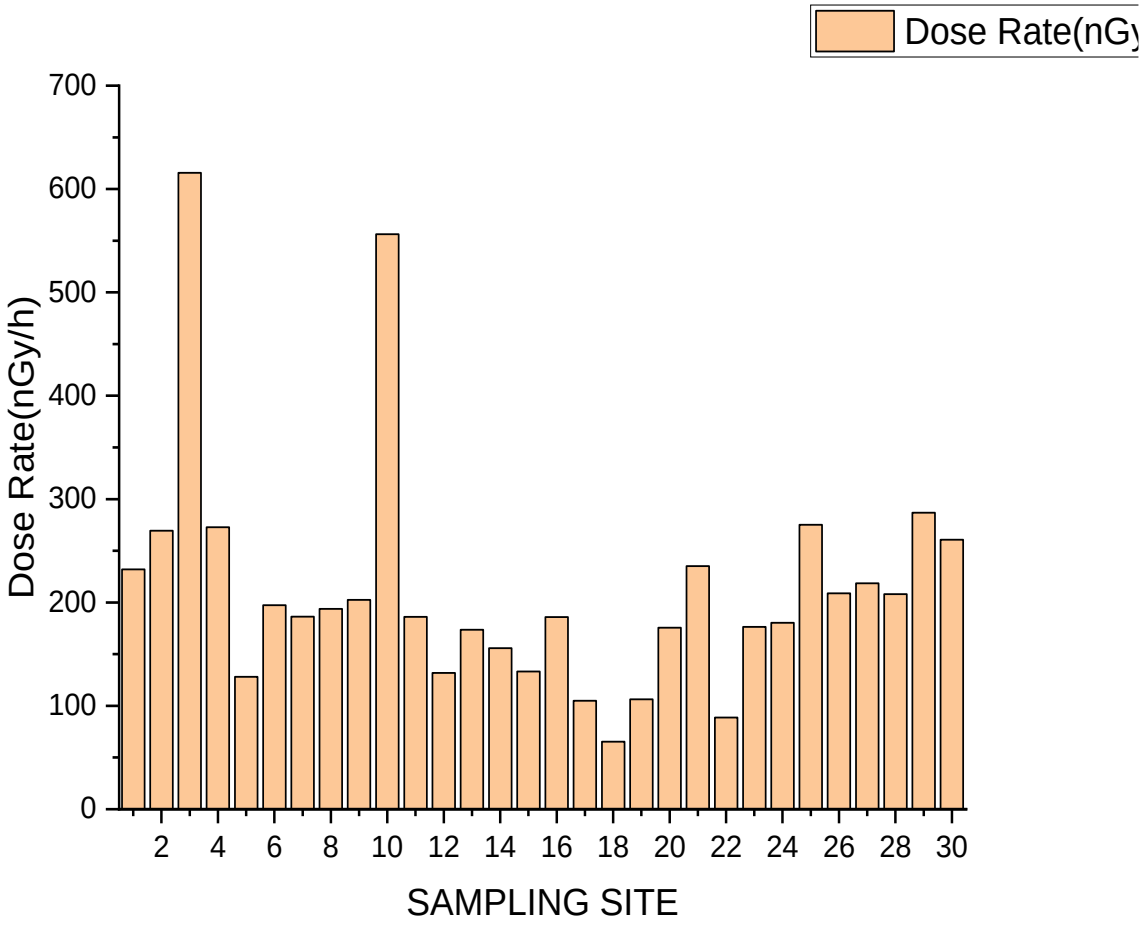

Figure 10: Dose rate from the building materials measured in the research work

5.2.1 Annual Effective Dose Rate

Equation (4.8) was employed to determine the annual effective dose rate, which ranged from 0.16 ± 0.006 mSvy^{-1} to 1.51 ± 0.014 mSvy^{-1}. The highest measurement was recorded in sample K3, surpassing the globally accepted maximum dose limit of 1 mSvy^{-1}. This elevated annual effective dose rate may be attributed to the samples being sourced from regions characterized by a significant presence of igneous rocks. The mean annual effective dose rate was 0.4323 ± 0.005 mSvy^{-1} which is relatively low in comparison to the dose limit of 1mSvy^{-1} (UNSCEAR, 2000).

Table 7: Annual effective dose rate for building materials collected along Kangundo

Sampling Site	Latitudes	Longitudes	AEDR (mSv/y)	Sample Type	Sample Origin
K1	36^0,65.1972’	01^0 ,10.758’	0.57 ± 0.01	Sand	Embu
K2	36^0,17.655’	01^0 ,55.324’	0.66 ± 0.01	Sand	Machakos
K3	36^0,57.677’	01^0 ,20.963’	1.51 ± 0.01	Sand	Kitui
K4	36^0,57.00’	01^0 ,20.963’	0.67 ± 0.01	Concrete	Kajiado
K5	36^0,54.390’	01^0 ,15.351’	0.31 ± 0.01	Concrete	Mulolongo
K6	36^0,57.343’	01^0 ,16.890’	0.48 ± 0.01	Sand	Kitui
K7	36^0,55.369’	01^0 ,15.437’	0.46 ± 0.01	Concrete	Mulolongo
K8	36^0,55.00’	01^0 ,15.430’	0.48 ± 0.01	Concrete	Mulolongo
K9	36^0,38.913’	01^0 ,15.751’	0.50 ± 0.01	Sand	Mai Mahiu
K10	36^0,58.606’	01^0 ,15.367’	0.53 ± 0.02	Sand	Narok
K11	36^0,59.517’	01^0 ,13.192’	0.46 ± 0.00	Brick	Kajiado
K12	36^0,00.370’	01^0 ,16.854’	0.32 ± 0.01	Sand	Mai Mahiu
K13	36^0,58.940’	01^0 ,14.765’	0.43 ± 0.01	Sand	Kitui
K14	36^0,58.827’	01^0 ,15.706’	0.38 ± 0.01	Sand	Machakos
K15	36^0,59.215’	01^0 ,15.885’	0.33 ± 0.01	Sand	Njiru
K16	36^0,58.2531’	01^0 ,18.465’	0.46 ± 0.00	Concrete	Kajiado
K17	37^0,01.565’	01^0 ,14.349’	0.26 ± 0.00	Sand	Mai Mahiu
K18	37^0,00.566’	01^0 ,16.833’	0.16 ± 0.01	Sand	Mwala
K19	37^0,01.291’	01^0 ,16.553’	0.26 ± 0.00	Sand	Masinga

K20	37^0,02.206’	01^0 ,16.992’	0.43 ± 0.00	Sand	Katani
K21	37^0,02.890’	01^0 ,17.064’	0.58 ± 0.00	Concrete	Thika
K22	37^0,03.484’	01^0 ,17.168’	0.22 ± 0.01	Concrete	Londiani
K23	37^0,03.919’	01^0 ,17.256’	0.24 ± 0.01	Brick	Londiani
K24	37^0,04.146’	01^0 ,16.917’	0.24 ± 0.00	Brick	Londiani
K25	37^0,04.612’	01^0 ,16.937’	0.39 ± 0.00	Brick	Mulolongo
K26	37^0,06.364’	01^0 ,17.115’	0.28 ± 0.01	Brick	Thika
K27	37^0,06.898’	01^0 ,17.088’	0.30 ± 0.01	Brick	Ruiru
K28	37^0,07.088’	01^0 ,17.161’	0.29 ± 0.01	Brick	Thika
K29	37^0,07.327’	01^0 ,16.564’	0.41 ± 0.00	Brick	Machakos
K30	37^0,08.307’	01^0 ,16.638’	0.36 ± 0.01	Brick	Ruiru

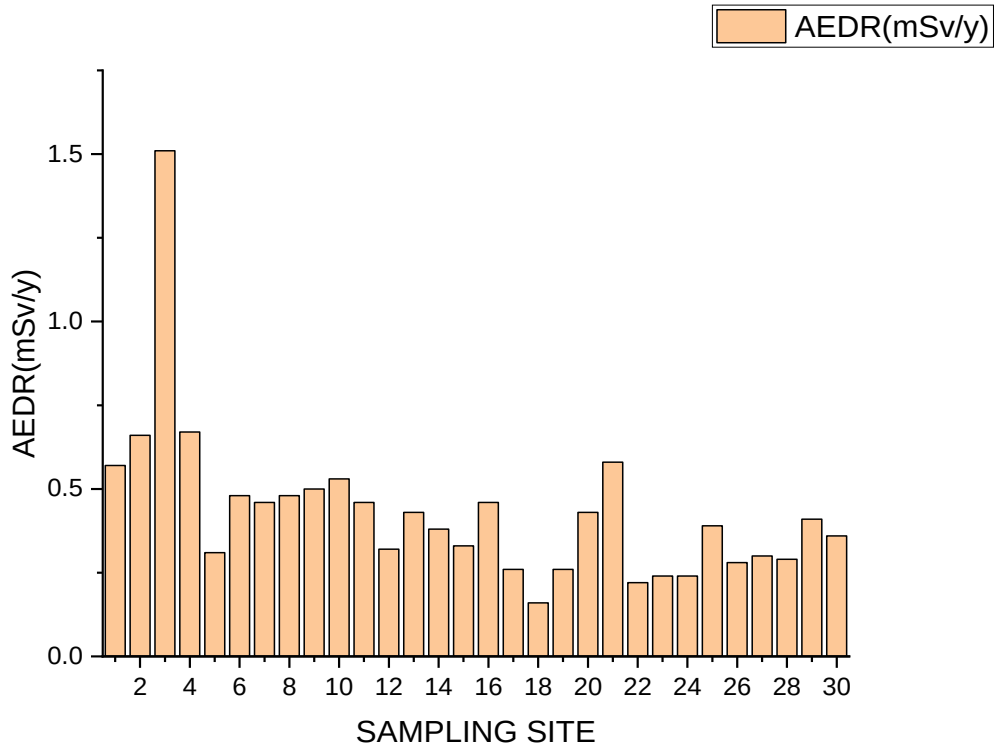

Figure 11: Annual effective dose rate for the samples of building materials.

5.2.2 Gamma Index

The computed Gamma index (Hazard Index) values for the samples varied, with a minimum of 0.31 ± 0.02 $mSvy^{-1}$ and a maximum of 3.63 ± 0.14 $mSvy^{-1}$, where six samples namely K1, K2, K3, K4, K10 and K21 exceeded the world permissible safety threshold of 1 $mSvy^{-1}$. The average Hazard Index was 1.01 ± 0.08 $mSvy^{-1}$ which is within the range of world permissible limit of 1 $mSvy^{-1}$ (UNSCEAR, 2000)

Table 8: The gamma index for randomized sample of building materials

Sample Site	Latitudes	Longitudes	Hazard Index (mSv/y)	Sample Type	Sample Origin
K1	36^0,65.1972'	01^0 ,10.758'	1.39 ± 0.06	Sand	Embu
K2	36^0,17.655'	01^0 ,55.324'	1.61 ± 0.07	Sand	Machakos
K3	36^0,57.677'	01^0 ,20.963'	3.63 ± 0.14	Sand	Kitui
K4	36^0,57.00'	01^0 ,20.963'	1.59 ± 0.07	Concrete	Kajiado
K5	36^0,54.390'	01^0 ,15.351'	0.75 ± 0.02	Concrete	Mulolongo
K6	36^0,57.343'	01^0 ,16.890'	1.11 ± 0.04	Sand	Kitui
K7	36^0,55.369'	01^0 ,15.437'	1.03 ± 0.04	Concrete	Mulolongo
K8	36^0,55.00'	01^0 ,15.430'	1.07 ± 0.04	Concrete	Mulolongo
K9	36^0,38.913'	01^0 ,15.751'	1.09 ± 0.04	Sand	Mai Mahiu
K10	36^0,58.606'	01^0 ,15.367'	1.22 ± 0.13	Sand	Narok
K11	36^0,59.517'	01^0 ,13.192'	1.03 ± 0.04	Brick	Kajiado
K12	36^0,00.370'	01^0 ,16.854'	0.77 ± 0.03	Sand	Mai Mahiu
K13	36^0,58.940'	01^0 ,14.765'	1.00 ± 0.04	Sand	Kitui
K14	36^0,58.827'	01^0 ,15.706'	0.85 ± 0.04	Sand	Machakos
K15	36^0,59.215'	01^0 ,15.885'	0.77 ± 0.02	Sand	Njiru
K16	36^0,58.2531'	01^0 ,18.465'	1.05 ± 0.04	Concrete	Kajiado
K17	37^0,01.565'	01^0 ,14.349'	0.6 ± 0.02	Sand	Mai Mahiu
K18	37^0,00.566'	01^0 ,16.833'	0.37 ± 0.02	Sand	Mwala
K19	37^0,01.291'	01^0 ,16.553'	0.61 ± 0.02	Sand	Masinga

K20	37^0,02.206’	01^0 ,16.992’	1.01 ± 0.04	Sand	Katani
K21	37^0,02.890’	01^0 ,17.064’	1.31 ± 0.05	Concrete	Thika
K22	37^0,03.484’	01^0 ,17.168’	0.50 ± 0.02	Concrete	Londiani
K23	37^0,03.919’	01^0 ,17.256’	0.58 ± 0.02	Brick	Londiani
K24	37^0,04.146’	01^0 ,16.917’	0.54 ± 0.02	Brick	Londiani
K25	37^0,04.612’	01^0 ,16.937’	0.91 ± 0.04	Brick	Mulolongo
K26	37^0,06.364’	01^0 ,17.115’	0.64 ± 0.03	Brick	Thika
K27	37^0,06.898’	01^0 ,17.088’	0.68 ± 0.03	Brick	Ruiru
K28	37^0,07.088’	01^0 ,17.161’	0.67 ± 0.03	Brick	Thika
K29	37^0,07.327’	01^0 ,16.564’	0.95 ± 0.04	Brick	Machakos
K30	37^0,08.307’	01^0 ,16.638’	0.85 ± 0.04	Brick	Ruiru

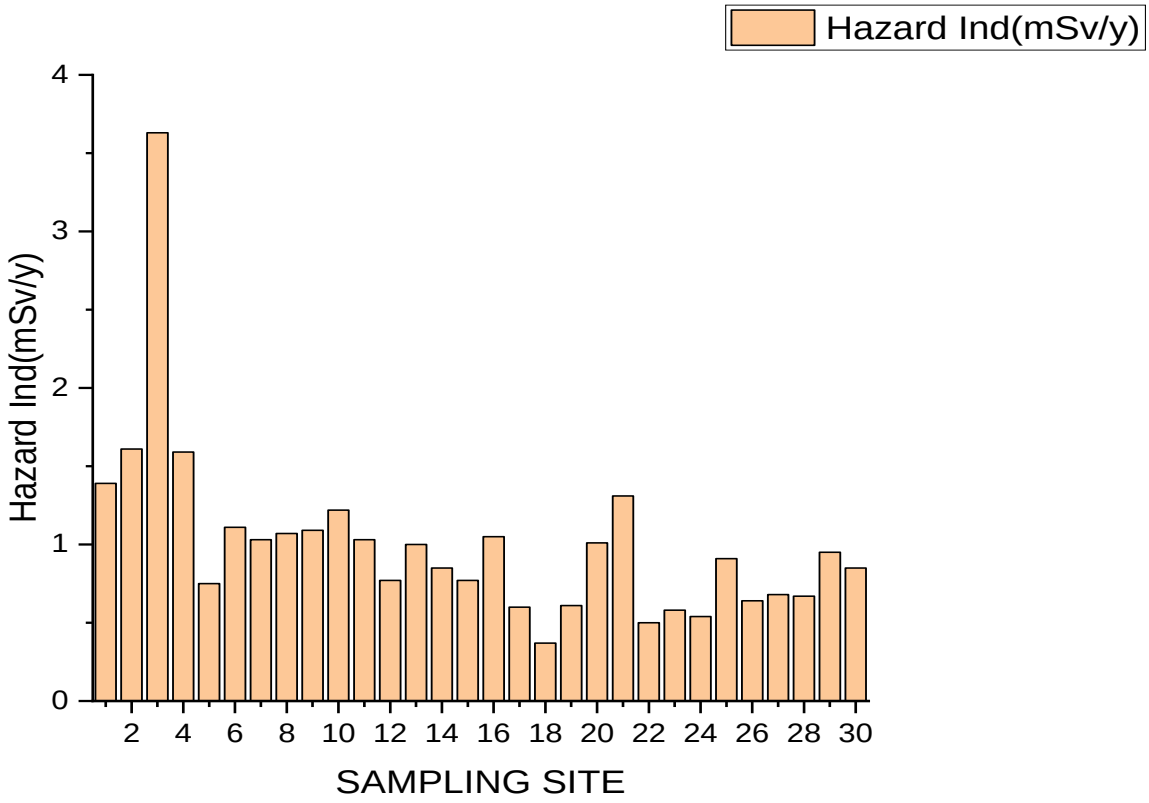

Figure 12: Gamma index for the building materials measured for this research work

CHAPTER SIX

CONCLUSIONS AND RECOMMENDATIONS

6.1 Conclusions

The research used gamma-ray spectroscopy in assessing the activity concentration levels for Natural Radiation Sources in building materials along Kangundo Road in Nairobi City County, Kenya. This research assessed the amount of radiation absorbed in the air (Dose rate), annual effective dose rate, radium equivalent activities and external hazard index in order to understand how gamma radiation affects human health and its effects on the surrounding environment. The reason for assessing the radioactivity levels as a prerequisite to estimate the radiological parameters is for the purpose of determining the ionizing radiation health effects due to human exposure to gamma radiation emanating from building materials. The resultant data was compared with global average values and standard acceptable limits. The levels of activity for ^{40}K ranged from 151 ± 8 to 2392 ± 120 Bq/kg, for ^{238}U from 27 ± 2 to 412 ± 21 Bq/kg, and for ^{232}Th from 54 ± 3 to 612 ± 31 Bq/kg. The mean radioactivity levels for the radionuclides exceeded the global average values of 420 Bqkg^{-1}, 33 Bqkg^{-1}, and 45 Bqkg^{-1} for ^{40}K, ^{238}U, and ^{232}Th respectively (UNSCEAR, 2000).

The average absorbed dose rate calculated was 214 ± 9 nGyh^{-1}. Which is below the world permissible safety limit of 1500 nGyh^{-1}. The average Radium Equivalent values were 374 ± 19 Bq/Kg which was within the world safety permissible value of 370 Bq/Kg except for Sample K3 with value 1343 ± 67 Bq/Kg.

Average Annual effective dose rate (AEDR) was 0.432 ± 0.005 $mSvy^{-1}$ which is below the world safety limit of 1 $mSvy^{-1}$ with a maximum value found in sample K3 which was above the maximum world permissible dose limit of 1 $mSvy^{-1}$. The study found that the building materials along Kangundo Road in Nairobi City County are safe for use in construction as they did not exceed the world admissible radiological parameter limits. Further research on samples of building materials such as sand from Kitui, which exhibited significantly elevated values of Hazard index and annual effective dose rate is required to determine the reason for the elevated radiation levels.

6.2 Recommendations

This research was carried out with a small number of construction materials collected at random from sites along Kangundo Road in Nairobi City County. It is thus advised to assess the radioactivity levels in samples with high AEDR and Hazard index values, such as K3, in locations where the construction materials were obtained. Determining the levels of radiation in construction materials is essential to verify the safety of the building materials on Kangundo road. Research on other building materials such as building stones not covered in this study should be done to determine the radioactive effects on human health and the environment. This will determine the chances and risks of individuals who are exposed to developing cancer or radiation related illnesses. The findings of this research will offer valuable information on radiation levels in construction materials that can be utilized by both the Kenya Nuclear

Regulatory Authority and the Nairobi County Government for decision-making and development of policy and guidelines for use of construction materials.

REFERENCES

Abdullahi, S., Ismail, A. F.and Yasir M. S. (2022). Radioactive investigation of Malaysia's building materials containing NORM and potential radiological risks analysis using RESRAD-BUILD computer code. *International Journal of Environmental Analytical Chemistry*, 102(9), 2000-2012

Achola, S.O. (2009). Radioactivity and elemental analysis of Carbonite rocks from parts of Gwasi area, *South West Kenya, M.Sc (physic) Thesis*, University of Nairobi.

Oborah,Amukah. (2022). Assessment of Radioactivity Concentration and Radiation Hazards Index for Building Materials Used in Babadogo Estate, Nairobi City County,*MSc Thesis KU.*

Amatullah, S., Rahman, R., Ferdous, J., Siraz, M. M. M., Khandaker, M. U.and Mahal, S. F. (2023). Assessment of radiometric standard and potential health risks from building materials used in Bangladeshi dwellings. *International Journal of Environmental Analytical Chemistry*, ***103*(14)**, 3376-3388.

Berekta, J., and Mathew, P. J. (1985). Natural Radioactivity of Australian building materials, *industrial wastes and by-products., Health physics* **48**:2509-2513.

Baykara, O., Sulikaratepe and Dogru M. (2000). Assessment of natural radioactivity and radiological hazards in construction materials used in Elazig, Turkey, *Radiation measurements* **30**:1-6.

Degu Belete and Alemu Anteneh*(*2021).General Overview of Radon Studies in Health Hazard Perspectives. *Journal of Oncology*.Volume 2021

Dunalp R.A (1988). Experimental physics. *Oxford University Press*, New York.11:12

Faheem, M., Mujahid S.A., and Mutiullah (2008). Assessment of radiological hazards due to the natural radioactivity in soil and building material samples collected from six districts of the Punjab province-Pakistan, *Radiation Measurement* **43**: 1443-1447.

Felix, K. Wanjala (2019). Human exposure to background radiation in Ortum, Kenya. *Journal of Radiation Protection Dosimetry* (2020, Vol. 188, No. 1, pp. 98–108.

Flores, O.B., Estrada, A.M., Sua'rez, R.R., Zerquera, J.T and Pe'rez, A.H (2005). Natural radionuclide content in building materials and gamma dose rate in dwelling in Cuba, *Journal of environmental radioactivity* **99-12:**1834-1837.

Gurisha, M. S., Makoba, A. A., Banzi, F. P.and Kiyengo, H. E. (2020). Determination of Natural Radioactivity Levels and Radiation Hazards from the Soil of Tin Mining in Kyerwa District, Tanzania.

Hashim N.O. (2000). The levels of radionuclides and trace in selected Kenyan coastal system. *M Sc. Thesis,* Kenyatta University.

Ibrahim, F. A., and Awadallah, I.M. (2009). Soil radioactivity levels and radiation hazard assessment in the highlands of Northern Jordan., *Radiation Measurement* **44(1):**102-110

International Atomic Energy Agency(IAEA). (2005). Analytical Tecniques in Uranium exploration and Ore prossing.Technical report, *International Atomic Energy Agency.No.341,81-99,IAEA,Vienna*

International Atomic Energy Agency(IAEA). (2005). Annual report (2011*), International Atomic Energy Agency.,IAEA,Vienna*

International Atomic Energy Agency(IAEA). (1987). Preparation and Certification of IAEA Gamma spectrometry reference materials. *International Atomic Energy Agency*. IAEA/RL/148, IAEA, Vienna in building materials available in Israel. *Building and Environment* **37**:531-537.

International Commission on Radiological Protection. (2000). Recommendations of International Commission on Radiological Protection.*ICRP Publication 60. Oxford: Pentagon press*

International Digital Organization for Science Information (2012). *Radiation online:www.idosi.org,Vol 9.November 2016.*

Khandoker A.,(2015). Assessment of Natural Radioactivity levels and potential Radiological Risks of common building materials used in Bangladesh dwellings website: *http://www.paperity.org*

Mann, W. and Gartinkil, S. (1966). Radioactivity and its measurement. *Van Nostrand-Reinhold, New York.*

Mavi, B. and Akkurt, I. (2010). Natural radioactivity and radiation hazards in some building materials used in Isparta, Turkey., *Radiation physics and chemistry* **79**:933-937.

Melissions, A. (1966). Experiments in modern physics. *Academic press,* New York **5**:45-59.

Mohan, S., & Chopra, V. (2022). *Chapter 18 Biological Effects of Radiation*. In Woodhead Publishing Series in Electronic and Optical Materials, Radiation Dosimetry Phosphors. *Woodhead Publishing. PP 485-508, ISBN 9780323854719. https://doi.org/10.1016/B978-0-323-85471-9.00006-3.*

Mustapha, (1999). Calculation of the radioactivity concentration of the radionuclide Using the Comparison Method., Applied *Radiation and Isotopes* **51**:93-96.

Nurgül Hafızo ˘glua, (2024). Efficiency and energy resolution of gamma spectrometry system with HPGe. *Department of Physics, Faculty of Sciences, Istanbul University, 34134 Vezneciler, Istanbul, Turkey.*

detector depending on variable source-to-detector distances

Okalebo, S.E., Mwasi, B., Musyoka, R., Karanja, N., Gachene, C., and Mwasi, S. (2009).” Green based” planning that integrates urban agriculture into Eldoret mixed landscape in response to climate change. School of Environmental Studies. *Moi University, Eldoret, Kenya.*

Osoro, M.K. (2007). Levels of natural radionuclides in surface soils around Titanum mines at Kenyan coast. *MSc (physics) Thesis, Kenyatta University*.

Procz *et al* (2019).X-ray and gamma imaging with Medipix and Timepix detectors in medical research*. Radiation Measurements. Volume 127, August 201*

Rotich C.K (2015) Gamma spectroscopic analysis of soil and green tea leaves of Kericho County. *MSc (Physics) Thesis, Kenyatta University.*

Simin, M., Reza, F. and Sedigheh, S. (2011). Natural radioactivity in building materials in Iran*. Nukleonik* **56**(4):363-368.

Songa, K. L. (2021). Analysis of Natural Radioactivity Levels and Radiation Hazards due

to Murram Quarried in Kakamega County, Kenya. *M.Sc.(Physics) Thesis, Kenyatta University*

Stojanovska, Z., Nedelkovski, D and Ristova, M. (2010). Natural radioactivity and human exposure by raw materials and product from cement industry used as building materials. *Radiation measurement **45**:969-972*.

Stoulos, S., Manolopoulou, M., and Papastetanou, C. (2003). Assessment of natural radiation exposure and radon exhalation from building materials in Greece. *Journal of environmental radioactivity* **69**: 225-240.

United Nations centre for human settlements. (2009). The Management of secondary cities in sub-Sahara Africa*: traditional and modern intuitional arrangements*. UN-HABITAT 42-83.

United Nations Scientific Committee on the Effects of Atomic Radiation. (UNSCEAR, 2008). Effects if ionizing Radiation. *Report of United Nations Scientific on effects of Atomic Radiations to the General assembly. United Nations, New York USA.*

United Nations Scientific Committee on the Effects of Atomic Radiation. (UNSCEAR, 2000). Sources and effects of Atomic Radiations. *Report of United Nations Scientific on effects of Atomic Radiations to the General assembly. United Nations, New York USA*.

United Nations Scientific Committee on the Effects of Atomic Radiation. (UNSCEAR, 1988). Sources and effects of Atomic Radiations. *Report of United Nations Scientific on effects of Atomic Radiations to the General assembly. United Nations, New York USA.*

Viresh K., Ramachinran, T.V, and Rasandra, P. (1999). Natural radioactivity of Indian building materials and by-products, *Applied Radiation and Isotopes* **51**:93-96.

WHO(2012). WorldHealthOrganization,IonizingRadiationinourEnvironment,online.***www.who.int/ionizing_radiation/env/en.(***accessed 17-6-2012).

XU et al (2020). Analysis of gamma-ray spectra with spectral unmixing. *Determination of the characteristic limits (decision threshold and statistical uncertainty) for measurements of environmental aerosol filters*

PLATES

PLATE A1: Map of Sampled Points along Kangundo Road

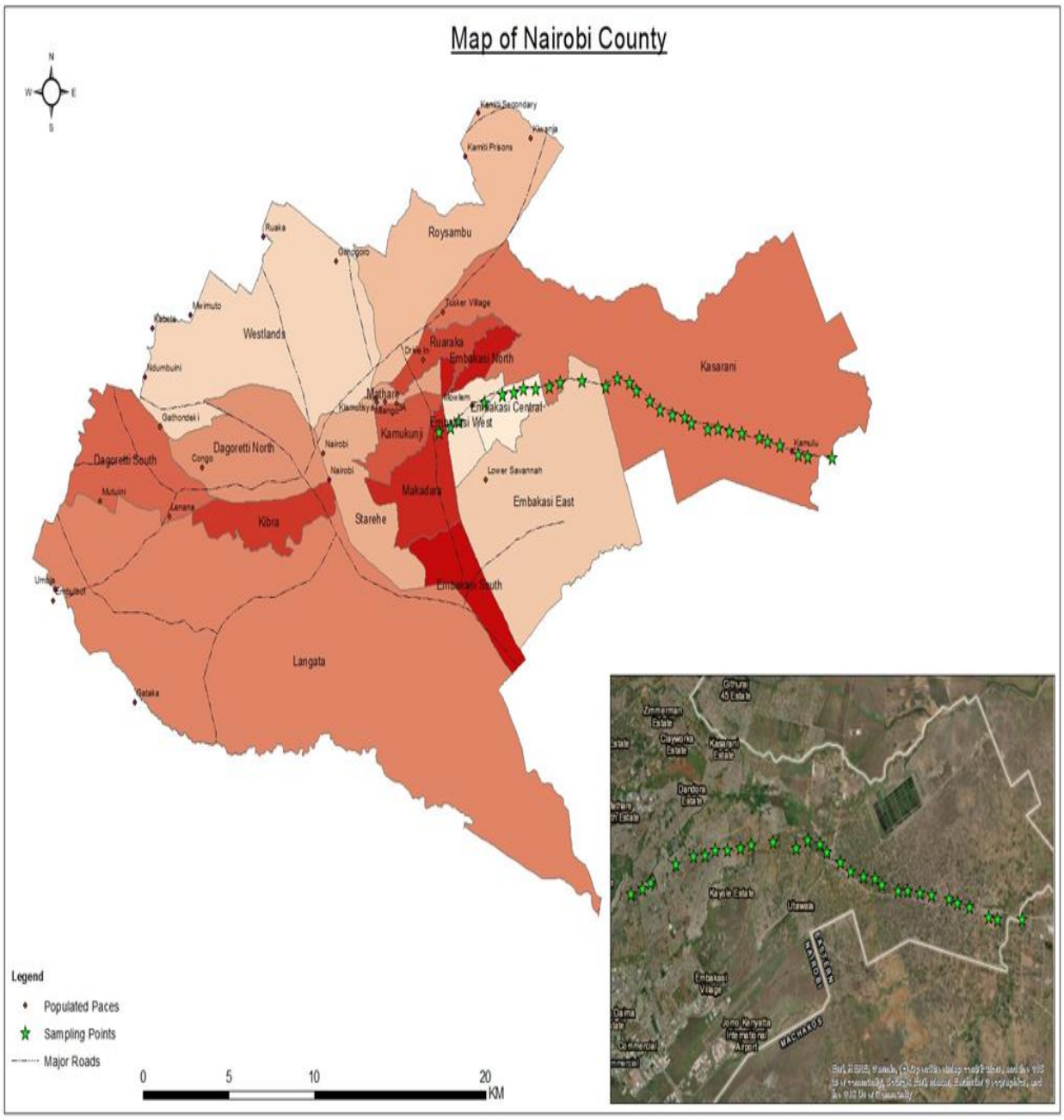

PLATE A2: A Screenshot Photo of sand Sampling Site

PLATE A3: A Screenshot Photo during Analysis of building materials in K.U Lab

APPENDICES

Appendix I

The IAEA reference sample's probability of emitting gamma rays (IAEA, 2005)

Reference sample	Gamma-ray energy(keV)	Emission probability	Source nuclide
RGU-1	186	0.033	^{226}Ra
	242	0.074	^{214}Bi
	295	0.187	^{214}Pb
	352	0.358	^{214}Pb
	609	0.446	^{214}Bi
	1120	0.149	^{214}Bi
	1765	0.123	^{214}Bi
RGTH-1	238	0.450	^{212}Pb
	338	0.123	^{228}Ac
	583	0.307	^{208}T1
	2615	0.360	^{208}T1
RGMIX	1460	0.110	^{40}K
	1765	0.161	^{214}Bi
	2615	0.360	^{208}T1

Appendix II: ^{235}U Disintegration Succession

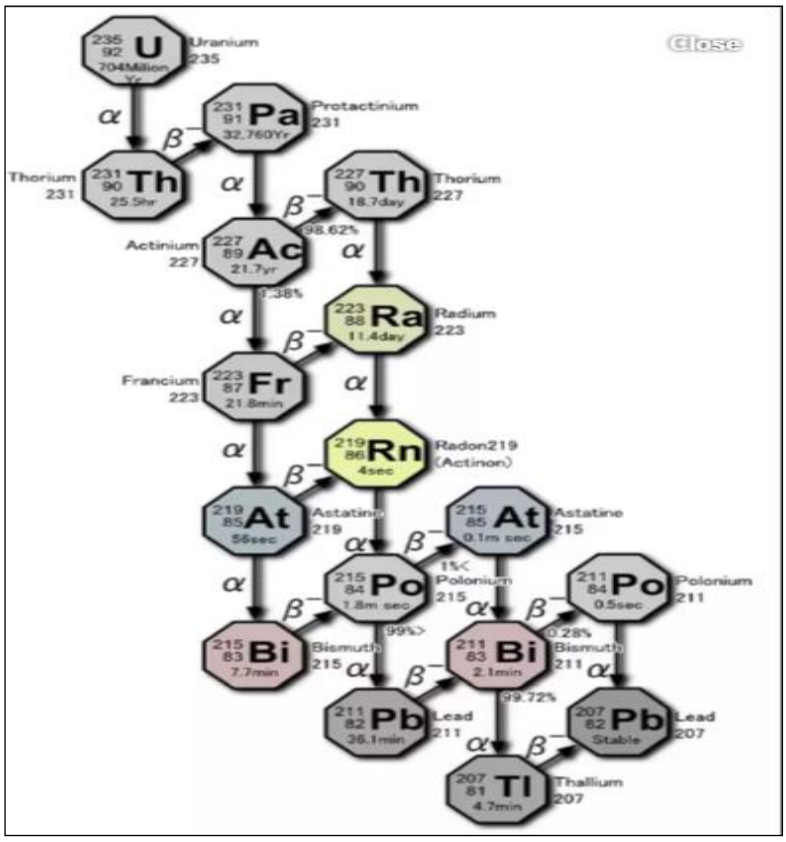

Appendix III: Endorsed Radiation Weighting Factor, WR

Radiation weighting factors (ICRP, 2000)

Radiation type	**Radiation weighting factor W_R**
Protons	2
Photons	1
Electrons	1
Alpha particles	0